Quantum Chemical Studies for the Mechanism of Phosphate Monoester Hydrolysis

By
Hammad Ali Hassan
NUST201361542MRCMS64213F

Research Centre for Modeling and Simulation
National University of Sciences and Technology
Islamabad, Pakistan
2016

Quantum Chemical Studies for the Mechanism of Phosphate Monoester Hydrolysis

By

Hammad Ali Hassan

NUST201361542MRCMS64213F

A thesis submitted in partial fulfillment of the requirement for the degree of Master of Science

in

Computational Science and Engineering

Research Centre for Modeling and Simulation
National University of Sciences and Technology
Islamabad, Pakistan
2016

Declaration

I hereby declare that this thesis comprises of my own research work; any part of this thesis is not plagiarized. The contributions of different people in the form of suggestions, discussions and previously published literature are acknowledged and duly referenced.

Hammad Ali Hassan

NUST201361542MRCMS64213F

Dedicated to my beloved Parents
and to my mentor Dr. Abid Nisar

Acknowledgements

God never spoils any effort. Every piece of work is rewarded according to the nature of devotion of it. I am humbly thankful to most gracious, merciful and ***Almighty ALLAH*** *who gave me healthy thought and talented teachers and helping friends and opportunity to complete my studies.*

I express my sincere gratitude to ***Dr. Ahmed Ejaz Nadeem****, Principal, Research Center for Modeling and Simulation (RCMS), National University of Sciences and Technology (NUST), for providing me a platform to do my research work under their expert guidance.*

I am greatly indebted to honorable ***Dr. Farooq Ahmad Kiani****, Associate Professor, RCMS, NUST, my research supervisor, for his empathy in many difficult situations. I am very thankful for his worthy suggestions, inspiring guidance and consisted encouragement without which this work would have never been materialized.*

I would like to be very thankful to all the GEC members: ***Dr Uzma Habib,*** *RCMS, NUST,* ***Dr Fouzia Malik****, RCMS, NUST,* ***Dr. Shumaila Sayyab,*** *RCMS, NUST for the continuous support and guidance.*

I am honored to thank my teachers at RCMS, ***AP Tariq Saeed****,* ***Dr. Salma Sherbaz*** *from the core of my heart for their stirring, lively and plentiful guidance in their respective subjects.*

I am very grateful to my friends Sohaib Aslam and Usman Yousaf, who supported and motivated me throughout my degree. I feel a deep gratitude to mention the names of Tauseef Mushtaq, Kashif Zahir, Muhammad Imran Nawaz and Muhammad Umair for sharing the best moments we have spent at RCMS. I am obliged to thank my valuable friends Shahid Mehmood,

Asif Shahzad, Muneeb Haider, Muhammad Ali Abbas, Muaz Aqeel for their encouragement throughout this tiring journey. We had a great time at NUST. I am very grateful to my fellows Mureed Hussain, Ali Malik, Muhammad Saad, Yasir Butt and Mr. Saqib for providing me support and quality time during my last days of research. Moreover, I am pleased to acknowledge my senior friends Mr. Sohail Khan and Mr. Adnan Khaleeq for their teaching and counselling during my MS degree.

I can't forget to mention my dear friend ***Umer Anayyat*** *for his moral support and worthy suggestions. I express my sincerest attitude to my best friend* ***Abeera Sikandar*** *for her well wished, outstanding company, cooperation, motivation and support during the course of study and throughout last eight years. I am very thankful to my* ***brothers*** *and* ***sisters*** *for their moral support and prayers. Additionally I am very thankful to my childhood friends* ***Azeem & Salman*** *for their encouragement. In the end I pay my best regards to my beloved* ***Parents*** *and sincerely acknowledge them for providing me the opportunity to earn this worthy degree.*

-Hammad Ali Hassan

Quantum Chemical Studies for the Mechanism of Phosphate Monoester Hydrolysis

ABSTRACT

Hydrolysis of phosphate containing compounds is important chemical reaction involved in many life processes such as DNA scission, cell division and organelle movement. Density functional theory calculations at M06-2X/6-31+G* and B3LYP/6-31+G** level of theory were carried out to calculate the mechanism of hydrolysis of phosphate monoester. For these calculations, two different starting set-ups of phosphate monoester, each differing with respect to the number of water molecules, were chosen. The stationary points along the potential energy surface that connect the reactant and the product structure were identified. The findings show that the energy barrier of the uncatalyzed hydrolysis of phosphate monoester in gas-phase is in the range of 37 to 48 kcal mol^{-1}. The mechanism of hydrolysis involves only a single water molecule. The stationary points along the minimum energy pathway of phosphate monoester hydrolysis involve the characteristics of both sequential (dissociative) as well as concurrent (associative) mechanisms. Adding explicit water molecule or the incorporation of implicit solvation model lower the energy barrier of hydrolysis.

TABLE OF CONTENTS

LIST OF FIGURES

LIST OF TABLES

Chapter 1
Introduction

1. Introduction

Phosphate containing compounds are the energy storehouse of life on earth.[1,2,3] Life processes such as cytokinesis,[4,5] organelle movement,[6,7] muscle contraction,[8,9] nucleic acid metabolism,[10,11] signaling,[12,13] protein synthesis,[14,15] biochemical cycles,[16,17] electron transport chain[18] reaction, phosphorylation,[19,20] and DNA replication[21,22] are all dependent on phosphate containing small compounds. Hydrolysis of phosphate containing compounds is the key chemical reaction. This is because their hydrolysis provides the energy required to execute most life processes.[23,24,25,26,27,28] In last two decades, there has been considerable progress in the computational studies for the hydrolysis mechanism of phosphate containing compounds.[29] Phosphate hydrolysis involves the breaking of two very strong bonds *i.e.*, one P–O bond of the substrate and one O–H bond of the attacking water molecule (Figure 1.1). Computational studies of phosphate hydrolysis have included a wide range of phosphate substrates, *i.e.* methyl phosphate,[30] methyl pyrophosphate,[31] adenosine triphosphate,[32,33] guanosine triphosphate[33] and methyl triphosphate[34] in vacuum,[31] solution,[35] and in protein.[12,14] Both standalone quantum mechanical[36] as well as combined quantum mechanical/molecular mechanical calculations[32,37] have been employed.

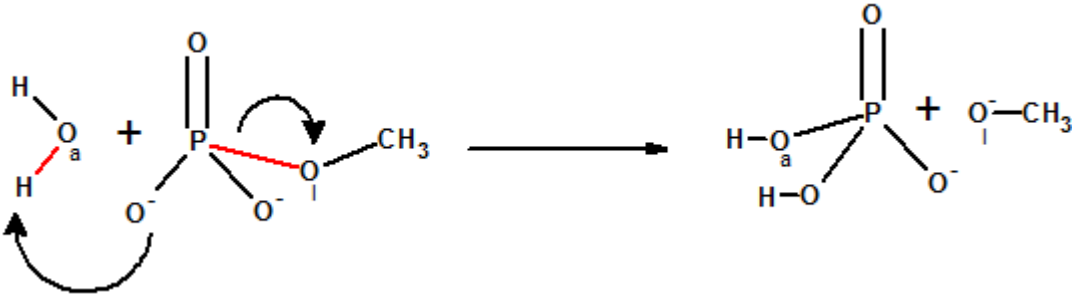

Figure 1.1 Hydrolysis of methyl phosphate requires breaking of two strong bonds, *i.e.* H-O$_a$ bond of water and P-O$_l$ bond of the methyl phosphate.

Computational studies in vacuum and in solution are helpful in understanding the phosphate hydrolysis mechanism in proteins. These studies have evolved over the passage of time, *i.e.*, gradually more accurate computational methods have been employed. Indeed a clear understanding of the mechanism of phosphate hydrolysis is still lacking. It is important to understand the controversial aspect of the previous mechanistic studies, which include a) The choice of reaction coordinates and the reaction mechanism and b) The mechanism of water splitting.

1.1 Choice of reaction coordinates and reaction mechanism

To describe the mechanism of hydrolysis reaction, different reaction coordinates have been used. Based on these reaction coordinates, the hydrolysis mechanism has either been referred to as a) one of the associative, dissociative or concerted mechanisms,[38] or b) a combination of associative and dissociative mechanisms[31] or c) sequential and concurrent.[36] Indeed this classification of mechanisms is dependent on the choice of reaction coordinates. The terms associative, dissociative and concerted have been used in very wide contexts, and have been very confusing.[35] These studies are discussed in detail in this section.

1.1.1 P–O_l and P–O_a distances in the transition state

The mechanism of phosphate hydrolysis has been traditionally studied using the distances of the P–O_l and P–O_a (see Figure 1.2).[31] Based on these reaction coordinates, hydrolysis reaction has been proposed to be either associative, when both P–O_l and P–O_a bond distances are short (Figure 1.2 A) or dissociative, when both P–O_l and P–O_a bond distances are long (Figure 1.2 B) in fully optimized transition state structures.[31,39]

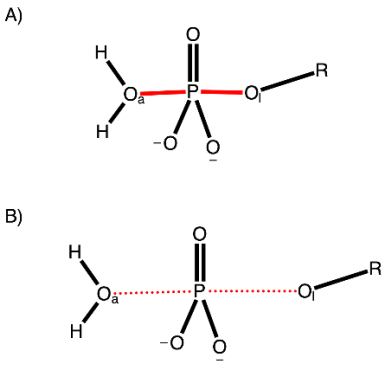

Figure 1.2 A) Trigonal bipyramidal transition state (with short P–O_a and P–O_l distances) is a typical associative transition state. B) Trigonal planar transition state (with long P–O_a and P–O_l distances) is a typical dissociative transition state.[31]

If the transition state structure contained both short P–O_l and P–Oa distances (trigonal bipyramidal transition state), the mechanism was considered as associative. However, if the P–O_l and P–O_a distances were larger (which clearly represented a dissociated case with trigonal planar metaphosphate transition state), the reaction was considered as dissociative. Depending on the type of mechanism, either associative or dissociative mechanism can be more favorable. Most recent computations have shown that hydrolysis reaction in most cases is neither associative (both P–O_l and P–O_a distances are short) nor dissociative (both P–O_l and P–O_a distances are long).

1.1.2 P-O_l and P-O_a distances as reaction coordinates

Another definition of the associative and dissociative mechanism is based on P–O_l and P–O_a distances as reaction coordinates. The reaction coordinates are plotted such that P–O_l bond breaking progresses along the x-axis, and P–O_a bond formation progresses along y-axis (Figure 1.3). In such a scenario, if P–O_l bond breaking occurs before the P–O_a bond formation, the reaction is considered dissociative (see red line in Figure 1.3). However, if the P–O_l bond breaking occurs after the P–O_a bond formation, the reaction is referred to as associative (see blue line in Figure

1.3). A middle line case is where P–O_a and P–O_l distances progress in such a way that a plot of the P–O_l bond breaking and P–O_a bond formation occurs concertedly (see diagonal black line).[38] A concerted mechanism indicates that both coordinates change in a coordinated fashion.

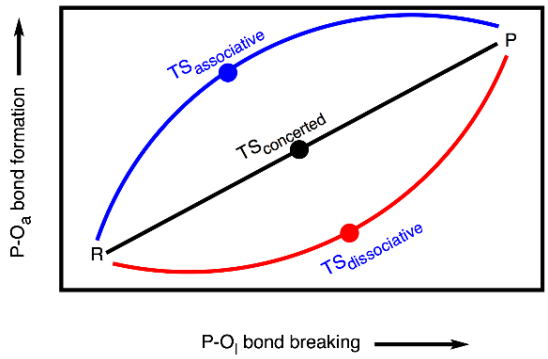

Figure 1.3 Progression of dissociative (red), associative (blue) and concerted (black) mechanisms[38]

1.1.3 P-O_l and O_a–H distances as reaction coordinates

More recently, reaction coordinates based on P-O_l and O_a-H distances have been used. Depending on whether O_a-H bond breaks before (Figure 1.4 A→B→ C→ D) or after the cleavage of P–O_l (Figure 1.4 A→E→D), the mechanism is regarded as sequential and concurrent, respectively. If the bond breaking event of P–O_l occurs before the bond breaking event of O_a-H, the mechanism is regarded as sequential. If H_2O_a attacks on phosphorous atom and breaking of P-O_l occur concurrently, the mechanism is referred as concurrent mechanism. Henceforth, in the following text of this thesis, the terms sequential and concurrent will be used to describe the hydrolysis mechanism, until and unless otherwise specified.[36]

1.2 The mechanism of water splitting

In addition to the unresolved aspect of the nature of the transition state and the type of transition state and reaction mechanism, it is also still controversial, whether hydrolysis occurs via

a single water molecule (Figure 1.4 A→E→D) or involves more than one water molecules (Figure 1.5 A→ B→C→D).

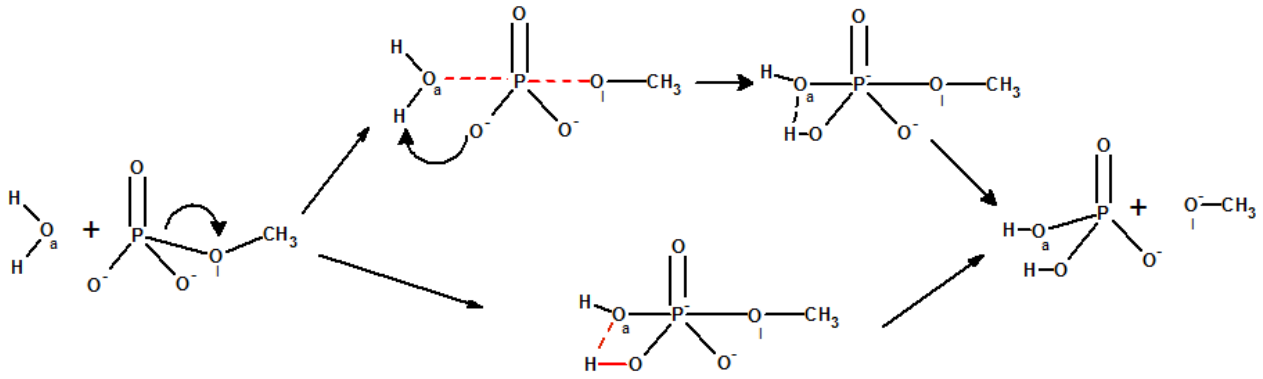

Figure 1.4 One water Sequential (B) and concurrent (E) transition states in phosphate hydrolysis

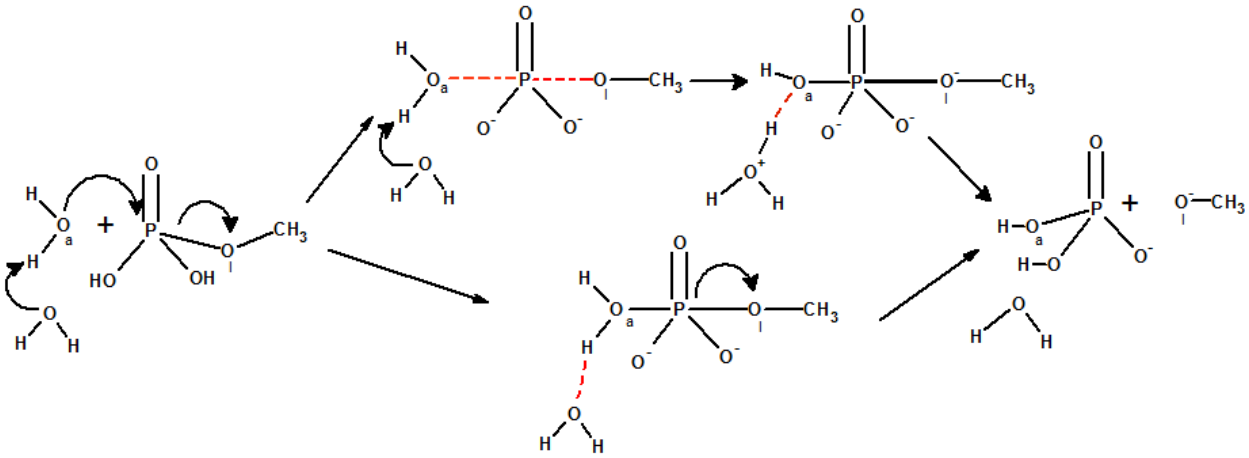

Figure 1.5 Two water Sequential (B) and concurrent (E) transition states in phosphate hydrolysis

1.3 Linkage types

Hydrolysis of nucleoside triphosphate (NTP), methyl triphosphate and methyl pyrophosphate involve in hydrolysis of P-O-P linkage, whereas in the case of methyl phosphate hydrolysis of P-

O-C linkage is involved. In all cases, in which hydrolysis of P-O-P linkage occurs, both one water as well as two water mechanism occur. However, in case of methyl phosphate, hydrolysis of P-O-C linkage occurs only by one water mechanism.[31]

1.4 Problem Statement

Phosphate hydrolysis is the key chemical reaction in biology. However, the mechanism of this apparently deceptively simple reaction is to-date not correctly understood. Quantum chemical simulations have proved to be crucial for understanding the reaction of phosphate hydrolysis at atomic details. But despite extensive work in last two decades, the details for the hydrolysis mechanism of phosphate-containing compounds are still conjectural: It has been reported that the hydrolysis mechanism of phosphate containing compounds can either be sequential or concurrent. Moreover, it can involve either one water mechanism or two water mechanism. In this study, by using quantum mechanical calculations at different levels of density functional theory (DFT), the mechanism of hydrolysis was studied to solve the mechanistic controversies, and find out the effect of implicit and explicit solvation on the mechanism of hydrolysis.

1.5 Aims and objectives of the study

The main objective of our study was to find out whether:

1. Hydrolysis of methyl phosphate occurs via a sequential or a concurrent mechanism, *i.e.* which type of transition state is involved in hydrolysis.
2. Preferred mechanism of hydrolysis in methyl phosphate involves a single water molecule or more than one water molecules and the effect of implicit and explicit solvent on the energy barrier of hydrolysis

Chapter 2
Literature Review

2. Literature Review

Hydrolysis of phosphate containing compounds has been studied by using quantum mechanical calculations in small reference compounds such as methyl triphosphate (MTP^{4-}),[40] nucleoside triphosphate (NTP^{4-}),[41] methyl pyrophosphate,[42] methyl phosphate,[43] as well as enzymes and molecular motors,[44] *e.g*. myosin, kinesin[45] and F_1-ATPase.[46] Selected cases of the non-enzymatic as well as enzyme-catalyzed[47] studies are reviewed to understand the hydrolysis mechanism of phosphate containing compounds.

2.1 Non enzymatic phosphate hydrolysis

Models of the non-enzymatic phosphate hydrolysis are important because a) these model reactions provide appropriate mechanistic details of the hydrolysis reaction in non-protein environment, b) their results are comparable with the experimental uncatalyzed reactions,[37] c) catalytic effect of protein environment can be estimated by comparing protein catalyzed reactions with these reference reactions, and d) modeling of non-enzymatic hydrolysis is computationally robust.

2.1.1 MTP^{4-} hydrolysis in solution

The hydrolysis of methyl triphosphate [48] ($MTP^{4-} + H_2O \rightarrow MDP^{3-} + H_2PO_4^-$) in solution[49,50] was studied by Nemukhin *et al.* in the absence of Mg^{2+} cation by using the effective fragment potential based using QM/MM method.[33] A sequential mechanism was observed in which first step was the breaking of P_γ–$O_{\beta\gamma}$ bond (see Figure 2.1 A) to produce an intermediate containing methyl diphosphate (MDP^{3-}) and a metaphosphate hydrate (PO_3^-. H_2O) (see Figure 2.1 C). The distance between O_a atom of H_2O_a and P atom of methyl diphosphate ($dO_{a\text{-}P}$) is 1.8 Å, whereas the distance between $O_{\beta\gamma}$ of methyl diphosphate and PO_3^- of metaphosphate ($dO_{\beta\gamma\text{-}P}$) is 3.1 Å. This intermediate is separated from the reactant structure via a transition state (E_{rel} = 20.0 kcal mol^{-1})

for P–O bond breaking, which has both $dO_{a\text{-}P}$ and $dO_{\beta\gamma\text{-}P}$ distances of 2.3 Å (Figure 2.1 B). Activation of attacking water molecule is carried out by a nearby helping water molecule W_{h1} that accepts a proton from the attacking water (Figure 2.1 B). This excess proton is later transferred to the ultimate proton acceptor, *i.e.*, ϒ-phosphate via a second helping water molecule (Figure 2.1 C and D). The energy of transition state structure for the formation of inorganic phosphate is 14.1 kcal mol^{-1}. They also computed corresponding concurrent mechanism for which the energy of the transition state structure was 35.1 kcal mol^{-1} (see Figure 2.2). Authors also compared the sequential MTP^{4-} hydrolysis in solution (Figure 2.1) with similar hydrolysis in RAS-GAP protein.[34] RAS-GAP in which MTP^{4-} is also complexed with Mg^{2+}, the metaphosphate intermediate has an energy of -2.0 kcal mol^{-1} relative to the reactant.

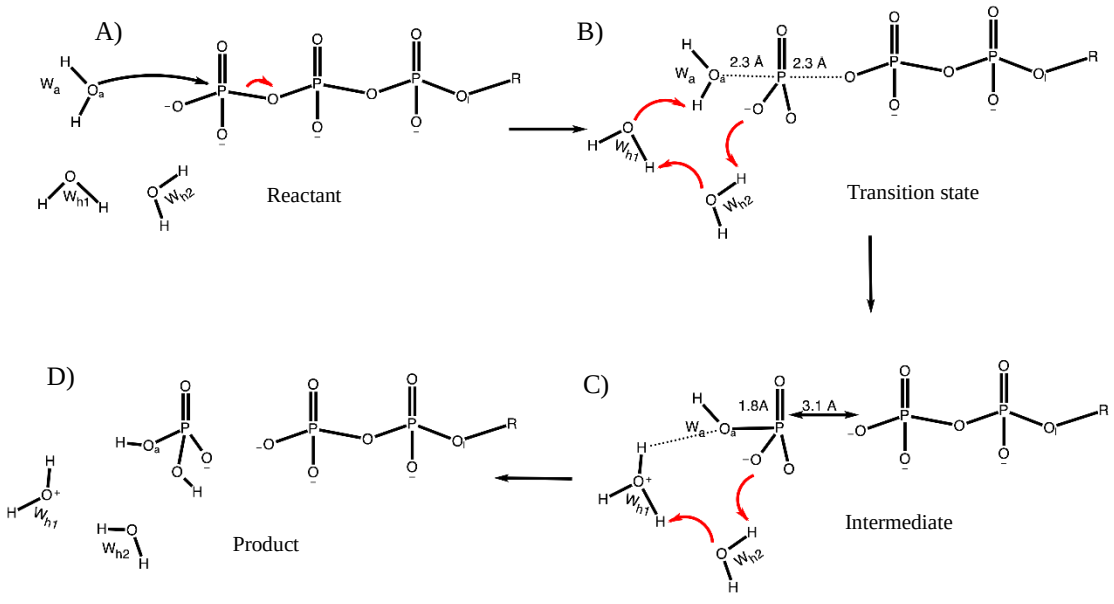

Figure 2.1 Sequential mechanism in the hydrolysis of methyl triphosphate[33]

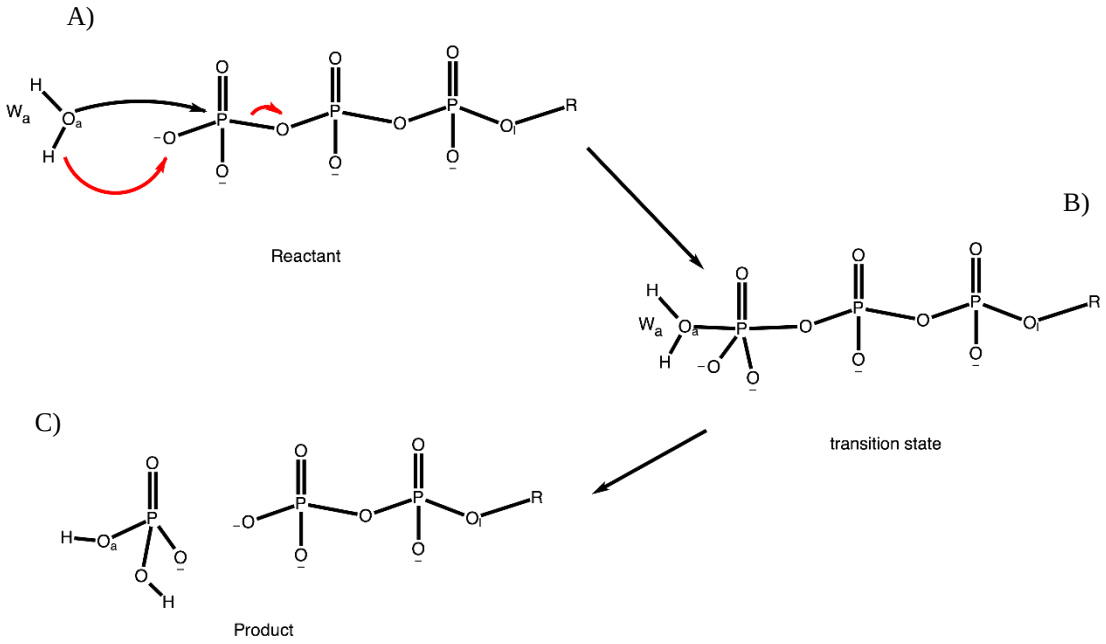

Figure 2.2 Concurrent mechanism in the hydrolysis of methyl triphosphate[33]

2.1.2 Nucleoside triphosphate hydrolysis in neutral and acidic solutions

The reaction of triphosphate hydrolysis is also studied by Glaves *et al.*[35] in neutral (Figure 2.3) as well as in acidic solution (Figure 2.4) using ab initio simulations. In both neutral as well as acidic solution, the methyl triphosphate is detached from diphosphate due to the P_γ-$O_{\beta\gamma}$ breaking as in the sequential mechanism. In the neutral case, two water molecules are involved in hydrolysis reaction (Figure 2.3 A): Initially the P-O_γ breaks and the attacking water attacks on phosphate (Figure 2.3 A and B). In the next step proton of attacking water molecule W_a transfers to W_h, which leads to the formation of H_3O^+ (Figure 2.3 C). Finally one of the proton on H_3O^+ transfers to the inorganic phosphate to form H_2PO_4 (Figure 2.3 D). On the other hand in acidic solution, four water molecules are involved (Figure 2.4 A), a) the excess proton on methyl triphosphate is transferred to one of the four water molecules and H_3O^+ is released (see the arrow between Figure 2.4 A and 2.4 B). b) OH^- of second water molecule, W_a, attacks on trigonal planar phosphate and H^+ shifts to

the oxygen of the phosphate (compare Figure 2.4 B, C and D). The end product of the reaction is $H_2PO_4^-$.

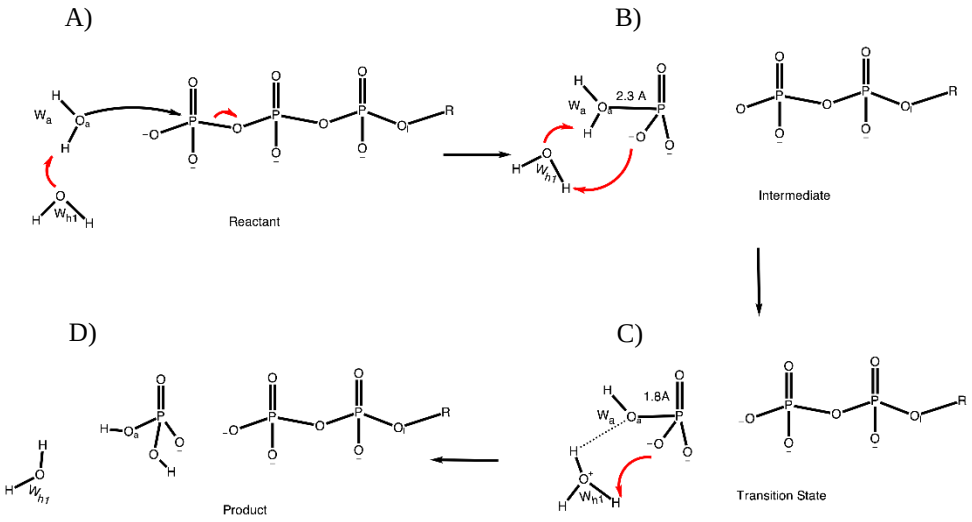

Figure 2.3 Two-water sequential mechanism of ATP hydrolysis in neutral solution[35]

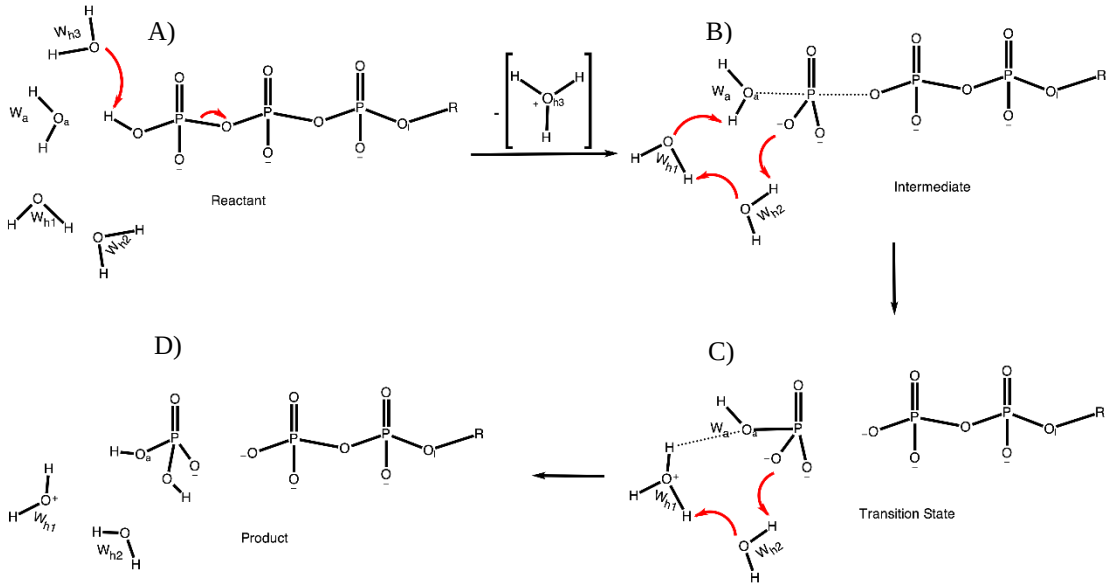

Figure 2.4 Two-water sequential mechanism of ATP hydrolysis in acidic solution[35]

2.1.3 Methyl pyrophosphate hydrolysis

Hydrolysis of monomethyl pyrophosphate trianion[51] has been computed by Warshel *et al.*.[52] They studied the one water approach in which a proton is directly shifted to the phosphate oxygen atom from the nucleophilic water (Figure 2.5 A→B→C→D). In the two water approach, the proton is transferred to the phosphate oxygen atom through a helping water molecule, which act as a shuttle for the proton transfer to the phosphate oxygen atom (Figure 2.5 A→ E→F→D). Terminal phosphate act as a base in the hydrolysis reaction. The sequential (Figure 2.5) or a concurrent mechanism (Figure 2.6) can occur either by one water or two water mechanism. In a sequential mechanism, the bond between phosphate and oxygen breaks before the nucleophile attacks of the attacking water (Figure 2.5). In the concurrent mechanism the attack of attacking water and the bond breakage of phosphate and oxygen occur at the same time (Figure 2.6).

2.1.4 Phosphate ester hydrolysis

The bond breaking and forming of phosphate plays a major role to pursue biological reactions. The phosphate bond cleavage occurs via hydrolysis. Florian and Warshel[53] have studied the hydrolysis of phosphate ester using OH^- ion.[53] OH^- is a fundamental element in the phosphate ester hydrolysis. OH^- attack breaks the P-O-C bond of the phosphate. In this study the authors only emphasized on the associated pathway of the phosphate ester hydrolysis. They studied on the monomethyl and trimethyl phosphate. When the OH^- attacks on the phosphate ester then in the meantime transfer of the proton to one of the oxygen of phosphate takes place. The energy barrier for monomethyl phosphate was 49 $kcalmol^{-1}$ and 44 kcal mol^{-1}. The impact of explicit water lowers the energy barrier from 49 to 37 $kcalmol^{-1}$ for monomethyl phosphate. The distances of the OH^- from phosphate in the transition state was 2.4 Å for monomethyl phosphate and 2.3 Å for trimethyl phosphate.[53] Later Warshel *et al.*[31] also compared associative mechanism with the dissociative mechanism of hydrolysis of phosphate ester. They studied the non-enzymatic hydrolysis of methyl

phosphates and found out two kinds of mechanisms which are associative and dissociative. They performed their studies on mono anionic, dianionic and neutral methyl phosphate. They concluded that both of the mechanisms are dependent on the distances between the P-O_a and P-O_l bond

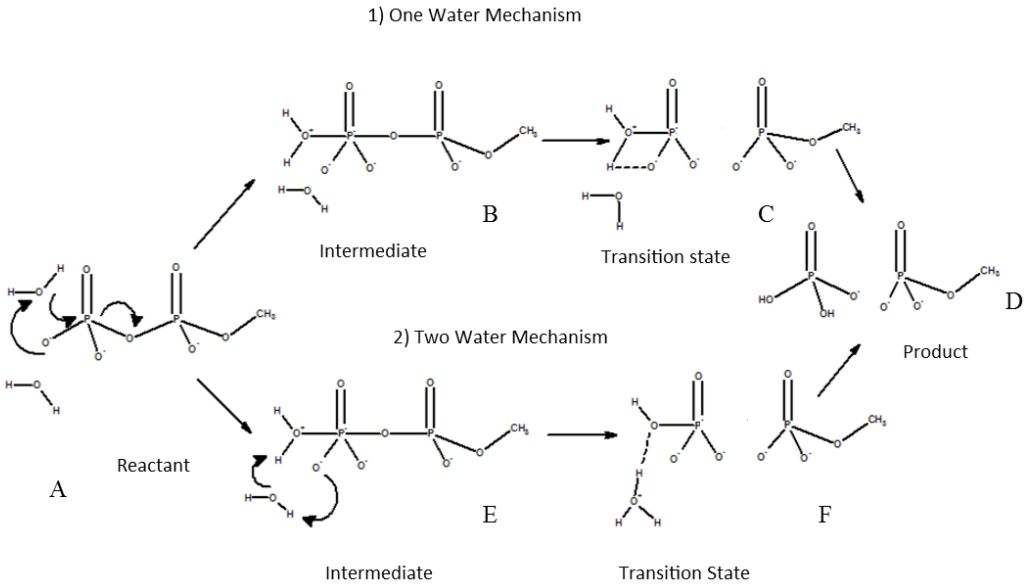

Figure 2.5 One and two-water sequential mechanism of methyl pyrophosphate hydrolysis[53]

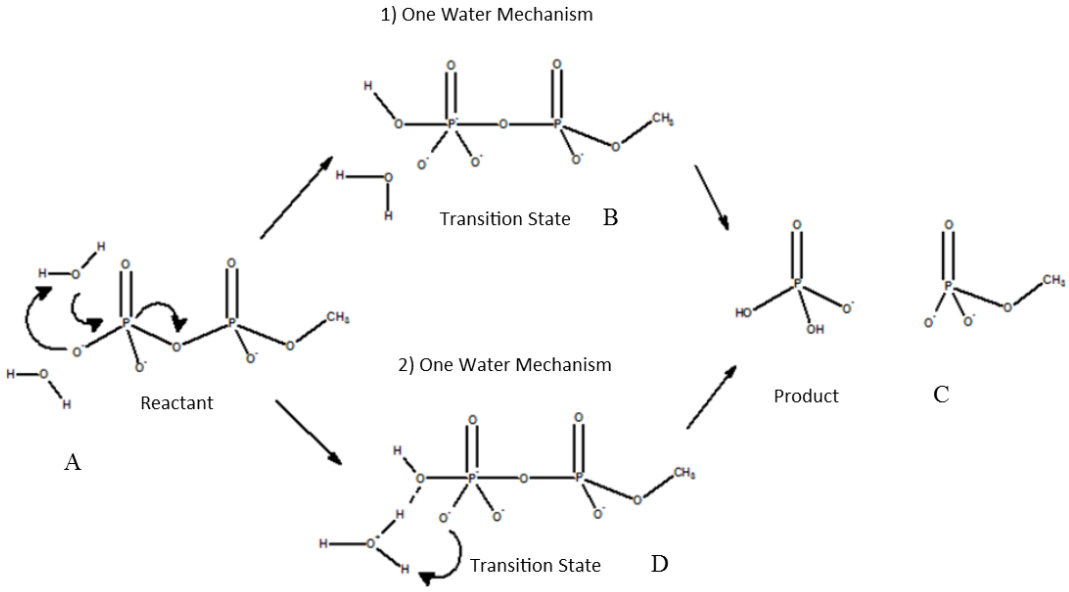

Figure 2.6 One and two-water associative mechanism of methyl pyrophosphate hydrolysis[53]

distances. For associative mechanism, the distance between the terminal phosphate and attacking water was 3.0 Å initially and in the transition state it was shortened to 1.66 Å. While the P-O_l distance was 1.67 Å initially and at TS2 it was extended to 2.23 Å. For dissociative mechanism, the distance terminal phosphate and attacking water was 3.00 Å and contracted to 1.97 Å˚ and the P-O_l distance was 1.67 Å initially and at TS2 it was extended to 2.00 Å. The energy barrier for associative mechanism was 26 kcal mol^{-1} and 44 kcal mol^{-1} for dissociative mechanism.[31]

2.1.5 Substrate assisted mechanism of p-nitro phenyl phosphate hydrolysis

The mechanism of phosphate hydrolysis is difficult to understand from decades. The mechanistic approach of phosphate hydrolysis on the free energy surface as studied by Kamerlin *et al.*[54] divides the mechanism into substrate assisted and solvent assisted. The distinct studies of phosphate monoester hydrolysis were performed on p-nitro phenyl phosphate (Figure 2.7) and methyl phosphate (not displayed). There are two kinds of reactions observed in Kamerlin *et al.* studies,[54] one is substrate assisted and other is solvent assisted. For the p-nitro phenyl phosphate the preferred mechanism of hydrolysis is solvent assisted. In this mechanism the proton transfer of the nucleophile is not direct. It occurs by the help of a water molecule which is present near P-O-C linkage. This interfering water molecule near the P-O-C linkage breaks the P-O-C bond and then the lytic water molecule or a nucleophile donates the proton to the oxygen of the phosphate. The pathway is energetically favorable with the average energy barrier of 26 kcal mol^{-1}. On the other hand, for the hydrolysis of methyl phosphate compound the preferred mechanism is substrate assisted with direct proton transfer of lytic water molecule occurs. The energy barrier for this mechanism is 38 kcal mol^{-1} which was further decrease to 28 kcal mol^{-1} when eight water molecules were added. The energy barrier of 20 kcal mol^{-1} is near to the experimental free energy

barrier of solvent assisted p-nitro phenyl phosphate. In both of the cases the addition of explicit water molecule plays an important role in the reduction of energy barriers.

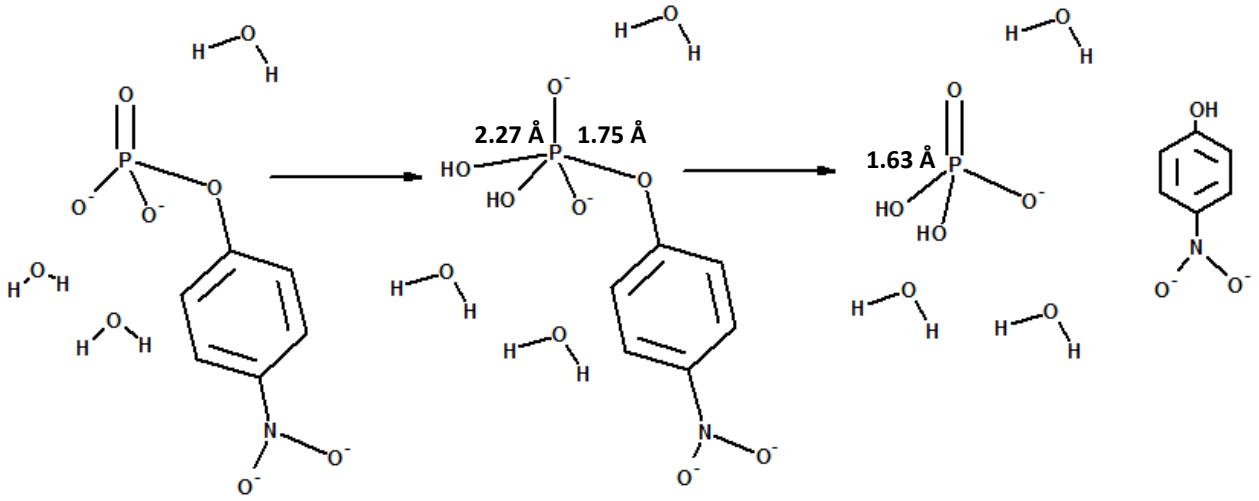

Figure 2.7 Substrate assisted mechanism of p-nitro phenyl hydrolysis[54]

2.2 Enzymatic Phosphate Hydrolysis

2.2.1 ATP hydrolysis in molecular motors

Molecular motors are the biological compounds that are responsible for all the cellular movements such as organelle movement, muscle movements, microtubules movements in cell division, nucleic acid synthesis mechanisms. Molecular motors use ATP as a source of energy for the movement. Considerable progress has been made in understanding the mechanism of ATP hydrolysis in molecular motors using QM/MM simulations. Simulations of ATPase enzymes suggested that the hydrolysis mechanism takes place by P_{γ}-O_{β} bond elongation. There is catalytic residue near the metaphosphate which helps nearby helping water to take the proton from the W_a water to form hydronium ion. Resulting OH^- attacks on metaphosphate, which leads to the hydrolysis product ADP.P_i. The proton from hydronium ion is abstracted and finally transferred to the ϒ-phosphate.

2.2.2 ATP hydrolysis in myosin

Molecular motor myosin hydrolysis[32,55] one molecule of ATP per one cycle of muscle contraction cycle. It undergoes an ATP hydrolysis reaction that starts with the dissociation of P-O bond of ATP (compare Figure 2.8 B with 2.8 A). The binding site of myosin contain two water molecules (W_a and $W_{h)}$ between Glu^{459} and the ϒ-phosphate. W_a is polarized by the catalytic setup consisting of W_h and Glu^{459} (Figure 2.8 B). Consequently it transfers one proton to the W_h. This results in the formation of hydronium ion (Figure 2.8 C). The extra proton of H_3O^+ then gets transformed to ϒ-phosphate that results in the formation of $H_2PO_4^-$ (Figure 2.8 C and D).[37]

2.2.3 ATP hydrolysis in F_1-ATPase

The mechanism of ATP hydrolysis in F_1-ATPase [56] has been studied by several research groups [57,58] using QM/MM simulations and single molecule observation experiments (The scheme is shown I Figure 2.9).[59] The overall reaction consist of bond rearrangement at the positions of ϒ-phosphate with $P_ϒ$ -$O_β$ bond dissociation (Figure 2.9 A and B) and proton transfer in the transition state region and Hydrogen Bonding rearrangements of water molecules in the binding pocket (Figure 2.9 C and D). These all stationary points have low activation energy as compared to alternate concurrent mechanism. In the intermediate state of (Figure 2.9 B), $P_ϒO_3^-$ is completely separated from the ADP^{3-}. The separated PO_3 interacts with the lone pair of the lytic water (W_a) to make its structure stable (Figure 2.9 B). As the distance between $P_ϒ$ –O_w bond decreased to 1.71 Å. The proton of W_a is released and transferred to the second water (W_h) (Figure 2.10 B). The second water molecule formed a hydronium ion. W_h releases a proton to Glu^{188}. The transferred proton at Glu^{188} relays to the ϒ-phosphate via W_3 by hydrogen bond rearrangement forming the product (Figure 2.9 D). The reaction occurs in a sequential manner.

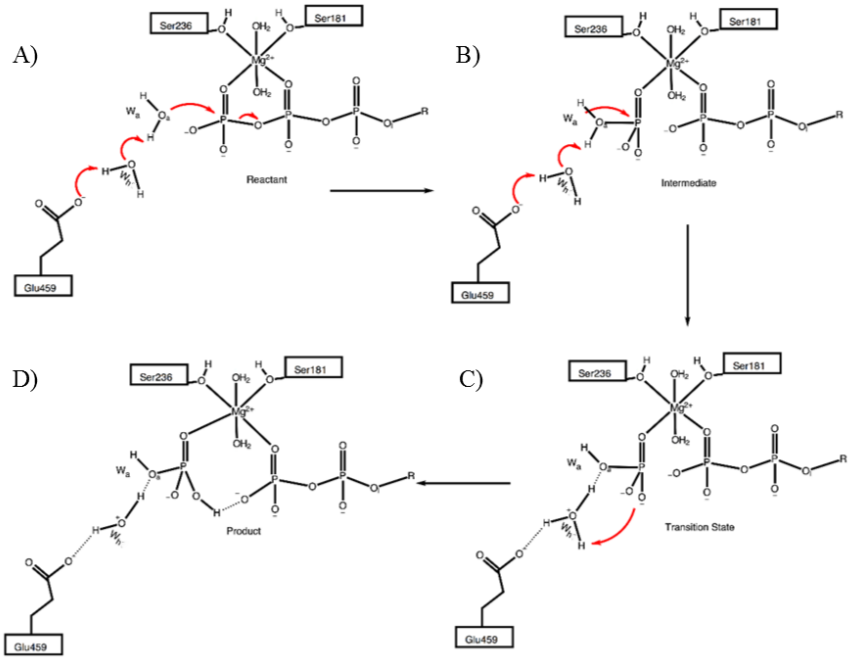

Figure 2.8 Sequential mechanism of ATP hydrolysis in molecular motor myosin[37]

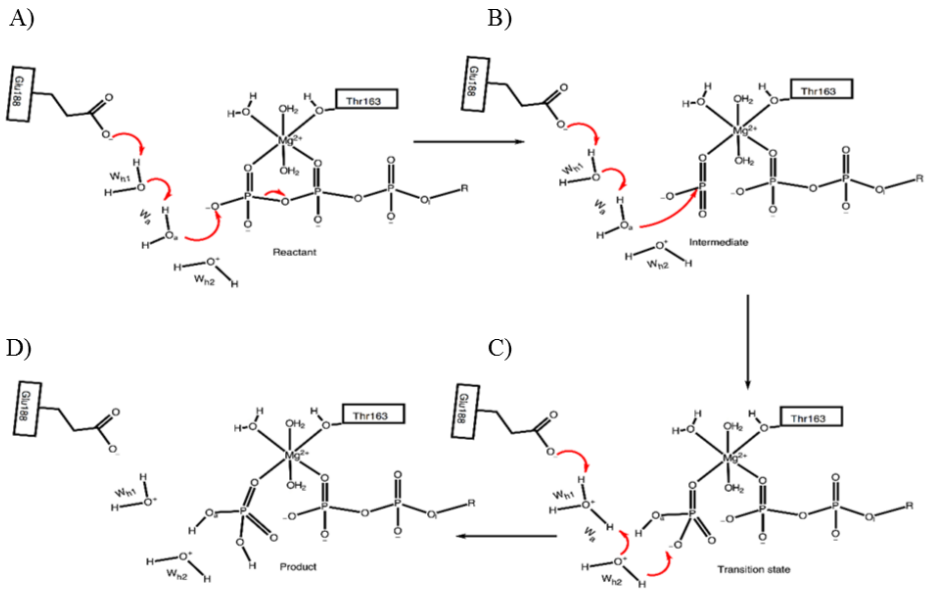

Figure 2.9 Sequential mechanism of ATP hydrolysis in F_1-ATPase[59]

2.2.4 ATP hydrolysis in kinesin

McGrath *et al.* proposed that ATP hydrolysis in kinesin occurs via two water molecule.[60] In the energetically most favorable hydrolysis reaction, the salt bridge was broken during entire simulation. Subsequently Glu^{270} acts as the transient proton acceptor and the final proton is transferred to Υ-phosphate. The product was more stable than the reactant. According to the studies of Parke *et al.*, the ideal state for the hydrolysis in NTPases is possible only when it is in closed state It has been observed that switch I regions of kinesin and myosin are closely related in adopting the confirmation changes, conformational changes leads the catalytic structure to undergo hydrolysis in closed state. The catalytic mechanism proceeds as follows: The attacking water W_a is positioned in a perfect manner from the Υ-phosphorous atom (Figure 2.10 A). The W_a water is surrounded by the switch I Ser^{223}, the amide group at the backbone Gly^{268} and a second water molecule W_a. Unlike nucleophilic W_a, W_h acts as proton acceptor. There are some key factors in the NTP hydrolysis which are as follows: the nucleophilic (W_a) that shifts its negative charge to the Υ-phosphate and there is (W_h) that acts as catalytic base and accepts the proton.

2.3 Challenges in the computation of hydrolysis reaction

2.3.1 Flexibility of small reference models:

Due to the absence of surrounding protein environment, these non-enzymatic models are much more flexible. This results in multiple minimum energy points on the potential energy surface.[34]

2.3.2 Choice of quantum mechanical method:

Choice of quantum chemical method greatly affects the energy barriers. For example, when Ma *et al.*.[61] changed quantum chemical method from SCF to MP2 for the hydrolysis of PO_3^--

$(H_2O)n$, the energy barriers reduced from 32 to 22 kcal mol^{-1} for n = 1, from 30 to 21 kcal mol^{-1} for n = 2, and

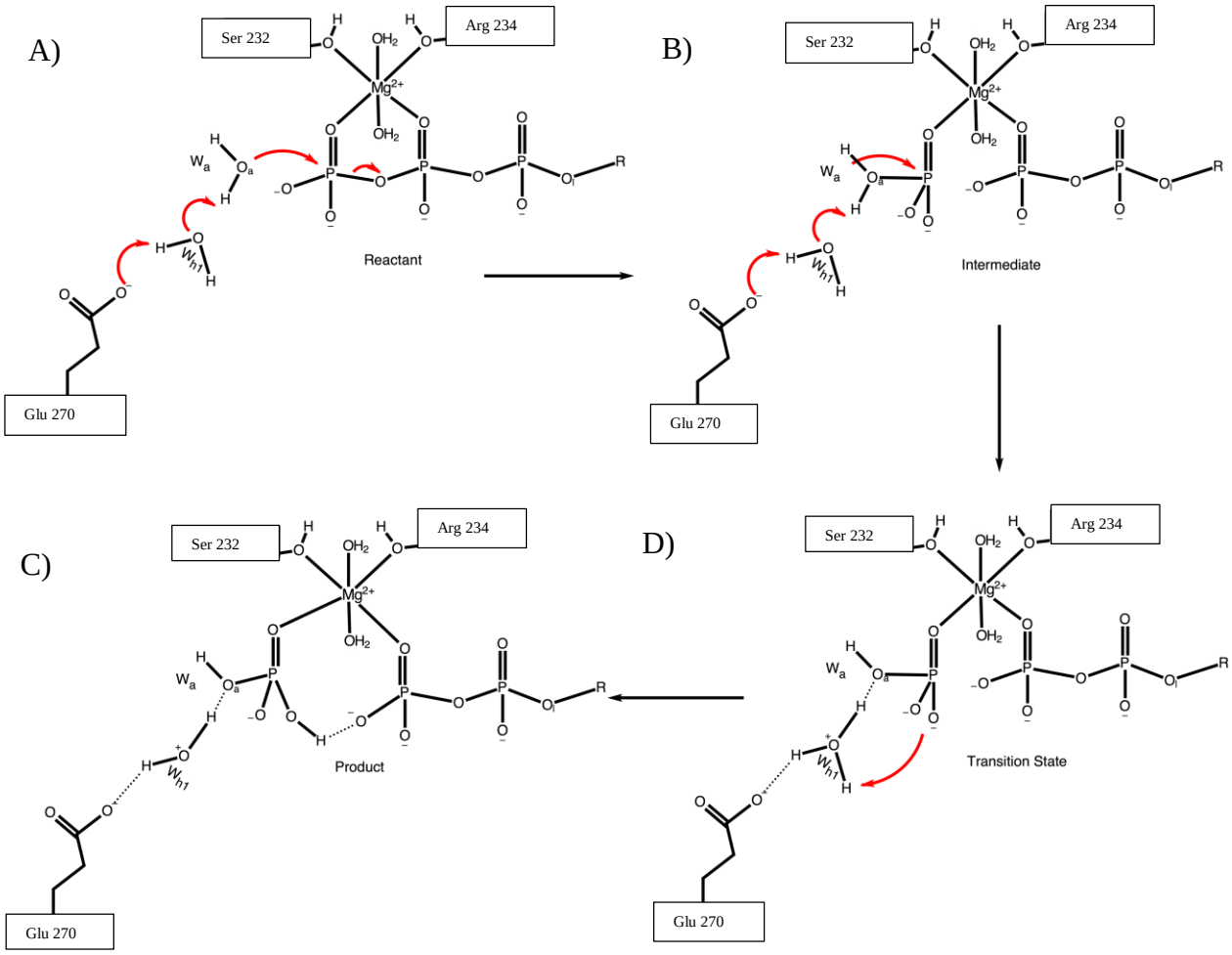

Figure 2.10 Sequential mechanism of ATP hydrolysis in kinesin[60]

from 30 to 21 kcal mol^{-1} for n = 3.[61] Nemukhin *et al.*[34] stated that the rate-limiting energy barrier of 20.0 kcal mol^{-1} for MTP^{4-} hydrolysis could be lower if they also computed the hydrolysis reaction at MP2 level of theory.[34]

From above literature review and the accompanied discussion it has become apparent that according to the previous studies a) triphosphate hydrolysis involves either a sequential or a concurrent mechanism b) it involves either a single water mechanism or a multiple water

mechanism c) both these water mechanisms have not been tested simultaneously for any methyl phosphate substrate d) different computational methodologies have been used which render the understanding of hydrolysis mechanism very difficult. Here computational investigation of phosphate hydrolysis mechanism tested and are reported in which a) the sequential and concurrent mechanism of hydrolysis were tested and b) one water and multiple water mechanism were also studied for methyl phosphate *i.e.* phosphate monoester.

Chapter 3
Methods

3. Methods

For Methyl phosphate (CH_3-O-PO_3^{2-}), geometries were optimized with M06-2X density functional [62] in combination with 6-31+G* basis set.[63,64,65] All presented structures are either a local minima or a first order saddle point on the M06-2X/6-31+G* potential energy surface. M06-2X is hybrid functional used to study the kinetics of transition states of compounds that contain main group transition elements. Normal mode analysis (frequency calculation) was performed to confirm that all optimized saddle points were of first order. The imaginary frequency obtained by the normal mode analysis were visualized using Molden software[66] to confirm that the obtained frequency corresponds to the desired saddle point between two local minima. Zero point vibrational energies from M06-2X/6-31+G* frequency calculations were included to derive the relative energies for all structures. Single point energies of all stationary points were calculated at M06-2X/6-31+G**. For selected single point calculation, PCM solvent model was used.[67] In addition reactant, product and transition state structures were also optimized on B3LYP/6-31+G**. All calculations were performed using parallel computing on the TCP-Linda environment on Linux-based supercomputer housed in the Supercomputing Research and Education Center (ScREC) of the Research Center for Modeling and Simulation (RCMS) at the National University of Sciences and Technology (NUST).

3.1Gaussian program package

Geometry optimizations and frequency calculations were carried out using the Gaussian 09 program, which is the latest updated software of Gaussian series. Gaussian provides computational tools to optimize geometries, minimizing structure of the transition states and their energies quiet efficiently.

3.2 Molden graphical interface

Molden[66] is software for displaying optimized geometries achieved by Gaussian, GAMES and semi-emperical packages of ampac/mopac. In Molden one can view the overall geometries and configurational changes taking place in the molecule from the option movie. Through the option of Z-matrix the geometries can be modified by changing the distances, angles of the structures.

3.3 GaussView

Gauss View is a software for viewing and editing geometries of molecules. The input file for the Gaussian 09 software can also be made in Gauss View. The finally build structure has also the property to use as an input file for Gaussian software.

3.4 Starting structures

Total two setups were made to study the hydrolysis mechanism for phosphate monoester. Following are the setups for phosphate monoester hydrolysis

a) Setup 1

b) Setup 2

a) Setup 1

The starting coordinates for our M06-2X gas phase optimization were obtained from those optimized on the free energy surface (in the presence of implicit as well as explicit water molecules) by Kamerlin *et al.*[54] The reactant structure contains two water molecules near the terminal phosphate (P_γ) and one near the P-O-C linkage. The structure of the reactant used in setup 1 is displayed in Figure 3.1. Two water molecules are located near the P_γ, whereas one water molecule is located near the P-O-C linkage.

b) Setup 2

The initial structure of Setup 2 has total four water molecules. Two water molecules near the terminal phosphate, one near the P-O-C linkage, one on the opposite side of oxygen number 2 (Figure 3.2). The addition of water molecules in setup 2 lowers the energy of all the stationary

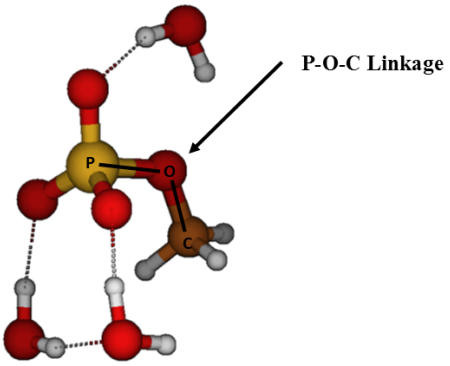

Figure 3.1 Optimized geometry of the methyl phosphate reactant as used in setup 1

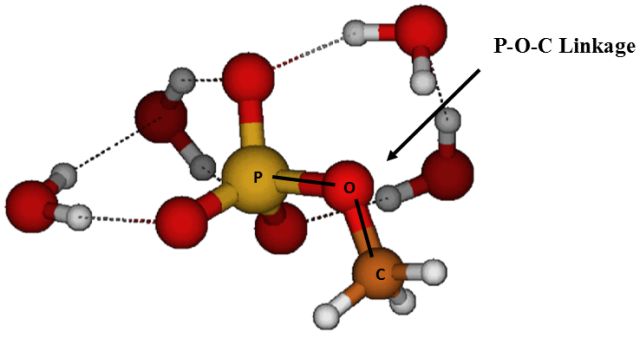

Figure 3.2 Optimized geometry of the methyl phosphate reactant as used in Setup 2

points along the potential energy surface as compared to setup 1. Like setup 1, the starting coordinates for M06-2X gas phase optimization were also obtained from those optimized on the free energy surface (in the presence of implicit as well as explicit water molecules) by Kamerlin *et al.*[54]

Chapter 4
Results

4. Results

The geometries of the reactant and transition state structures, intermediates and the final product were optimized on the potential energy surface by using the M06-2X/6-31+G* and B3LYP/6-31+G** methods. The geometries of Reaction 1 (for setup 1) and Reaction 2 (for setup 2) were optimized with M06-2X/6-31+G* as well as with B3LYP/6-31+G** will be presented.

4.1 Reaction 1 and Reaction 2 optimized with M06-2X/6-31+G*

4.1.1 Reaction 1

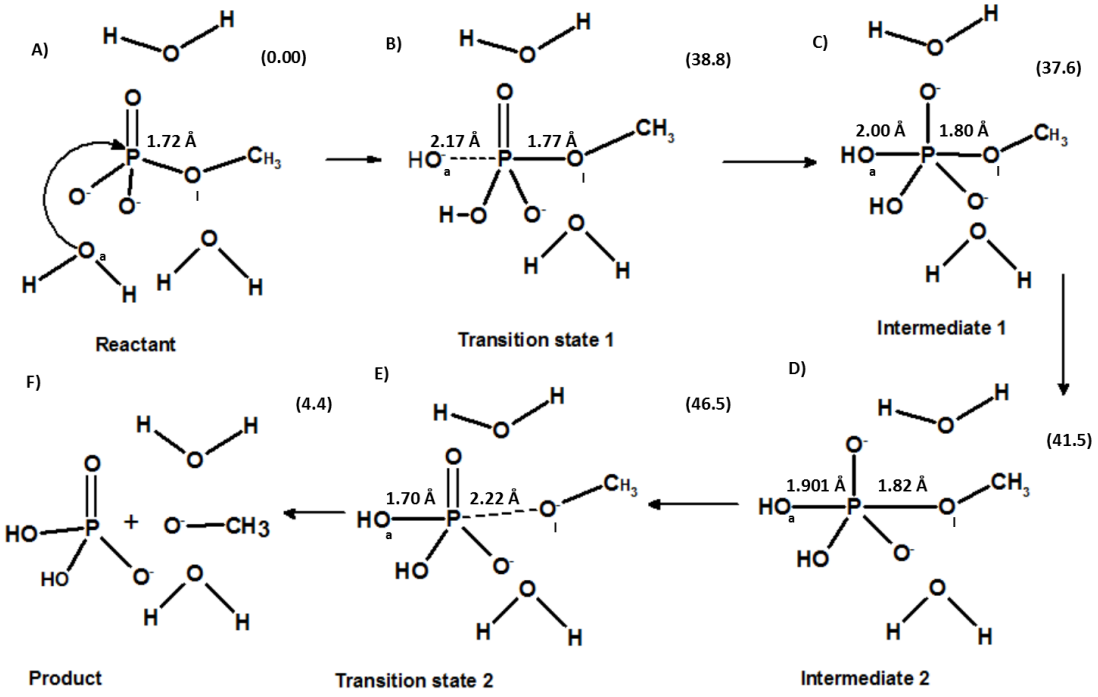

Figure 4.1 Reaction Scheme of Reaction 1, Values in parenthesis are energy values in kcal mol^{-1} relative to the reactant

In Reaction 1, the initial reactant structure, which contains two water molecules near terminal phosphate and one water molecule near the P-O-C Linkage is shown in Figure 4.1 A. Only one water molecules, which is an attacking water molecule (W_a) is involved in the hydrolysis and two

other water molecules are for the stability of the overall setup. The lytic water molecule attacks on the phosphate and transfers a proton to Υ-phosphate in a single step (Transition state 1). In the transition state 1 (B, Figure 4.1 and 4.3) the bond of the leaving oxygen O_l is still formed. The distance between the O_a-H and the P_Υ is 2.17 Å whereas the distance between O_l-CH_3 and P_Υ is 1.77 Å. The energy of the structure B is 38.8 kcal mol^{-1} relative to the starting reactant structure A. The next structure in the energy profile is an intermediate (Structure C in Figure 4.1 and 4.3). In this structure both P-O_a and P-O_l distances are 2.00 Å and 1.80 Å, respectively. This structure has an energy of 37.6 kcal mol^{-1} as compared to reactant. Indeed the intermediate 2 (Structure D) is structurally very closely related to the intermediate 1. It has P-O_a and P-O_l bond lengths of 1.90 and 1.82 Å, which is very close to the P-O_a and P-O_l bond lengths of intermediate 1. Its relative energy is 41.5 kcal mol^{-1}.

Reaction 1 proceeds by P-O_a bond formation and P-O_l bond breaking (Figure 4.2 and 4.5). The distance between the P-O_a bond gets shorter and the distance between P-O_l bond gets longer as the reaction proceeds from reactant to product.

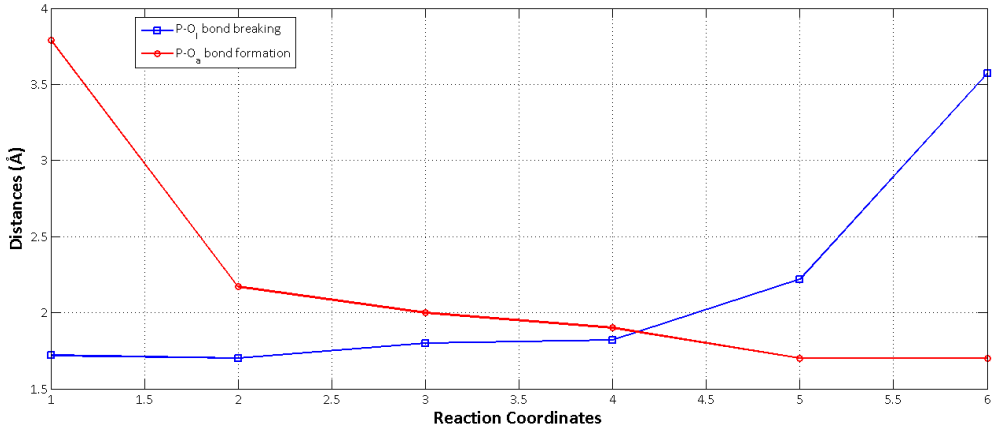

Figure 4.2 P-O_a and P-O_l bond distances of Reaction 1 from reactant to product

It is understandable that two intermediates are lying very close to each other on the energy plateau and probably the energy surface is flat enough that the energy barrier between the two intermediates are so much negligible that it could not be detected despite very carefully calibrated attempts to find such a transition state structure. P-O-C bond breaks at the same time as it is seen the Transition state 2 and the product is a methoxide, CH_3OH and monophosphate, H_2PO_4. The reaction 1 has concurrent pathway of hydrolysis.

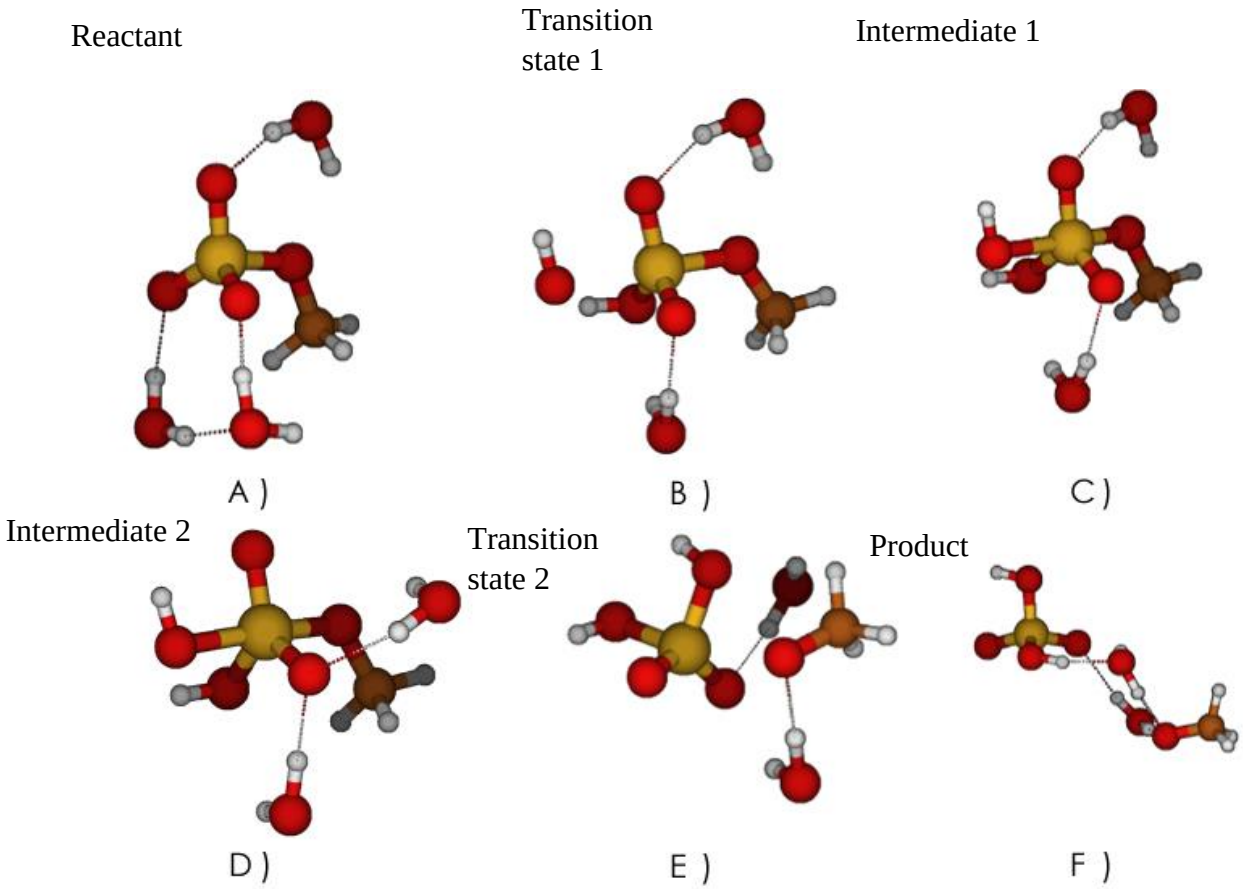

Figure 4.3 Optimized geometries of Reaction 1, A) Reactant B) TS1 C) INT1 D) INT2 E) TS2 F) Product

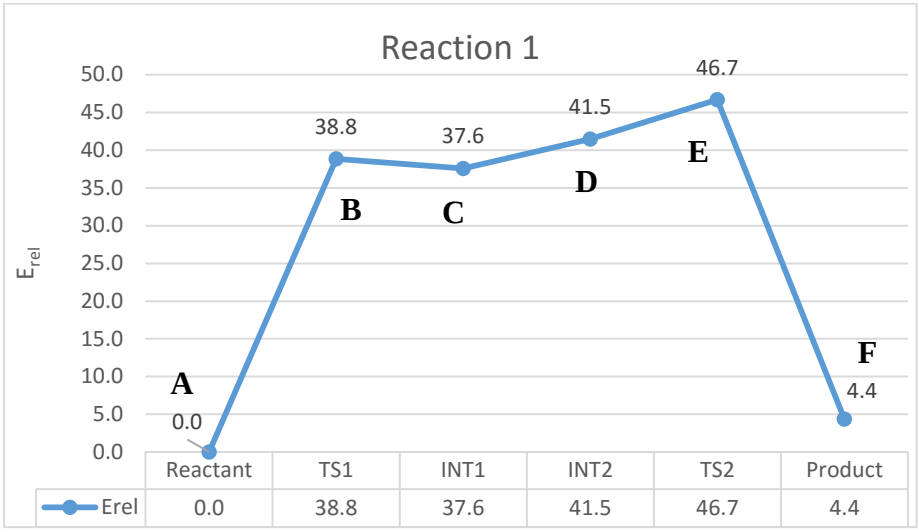

Figure 4.4 Energy profile of Reaction 1

The reaction profile of Reaction 1 has E_{rel} on y-axis and reaction coordinates on x-axis. All energies are relative to the reactant. TS1 has the energy of 38.8 kcal/mol and the rate limiting energy barrier for Reaction 1 is 46.7 kcal mol^{-1}. The 1st intermediate structure (INT1,C) has the energy of 37.6 kcal mol^{-1} and second Inermediate (INT2,D) has 41.5 kcal mol^{-1}. The final product with a very low energy of 4.4 kcal mol^{-1} . The progression of Reaction 1 according to Warshel *et al.*[38] studies shown in Figure 4.5.

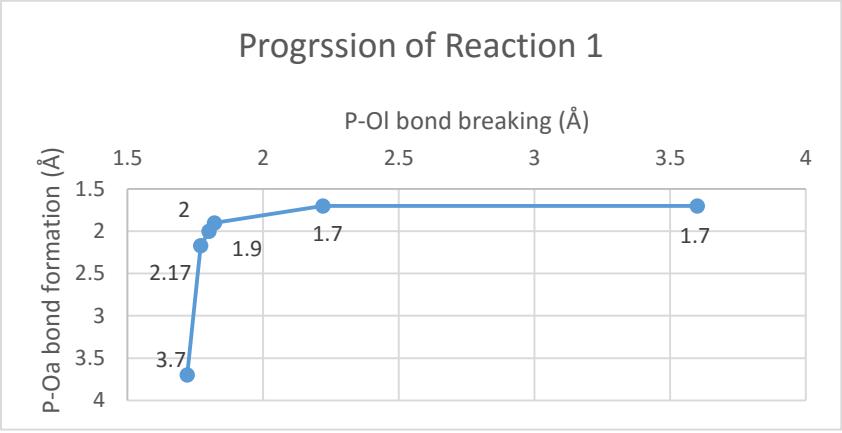

Figure 4.5 Progression of Reaction 1

Table 4.1 Energies (E_{rel}) relative to the reactant of all stationary points along Reaction 1 on M06-2X/6-31+G* energy surface.

Label	Stationary Points	Nimag	E_{opt}[a] (Hartree)	E_{opt}[b] (kcal mol^{-1})	E_{zpe}[c] (kcal mol^{-1})	$E_{opt}+E_{zpe}$[d] (kcal mol^{-1})	E_{rel}[e]
A	Reactant	0	-911.3	-571866.0	81.6	-571784.4	0.0
B	TS1	1	-911.3	-571827.1	81.3	-571745.8	38.8
C	INT1	0	-911.3	-571828.4	82.3	-571746.2	37.6
D	INT2	0	-911.3	-571824.5	81.9	-571742.6	41.5
E	TS2	1	-911.3	-571819.3	80.5	-571738.8	46.7
F	Product	0	-911.3	-571861.6	82.2	-571779.4	4.4

4.1.2 Reaction 2

The setup 2 differs from the setup 1. There are four water molecules in the setup. All the stationary points obtained along the potential energy surface are schematically presented in Figure 4.6, whereas optimized geometries shown in Figure 4.8.

As in Reaction 1, only one water is involved in the hydrolysis reaction which is located near the terminal phosphate. The lytic water molecule attacks from the front. In the first transition state, the O-H of the lytic water undergoes scission. Consequently, OH^- of the lytic water makes bond with the phosphate (compare B with A in Figure 4.6 and 4.8).

[a] The energy of optimized structures is in Hartree units.
[b] The Hartree energy was converted to kcal mol^{-1}
[c] E_{zp} is a zeropint energy which is calculated for vibrational frequencies
[d] E_{zp} added to E_{opt}
[e] $E_{zp} + E_{opt}$ of all structures in reaction 1 relative to that of reactants

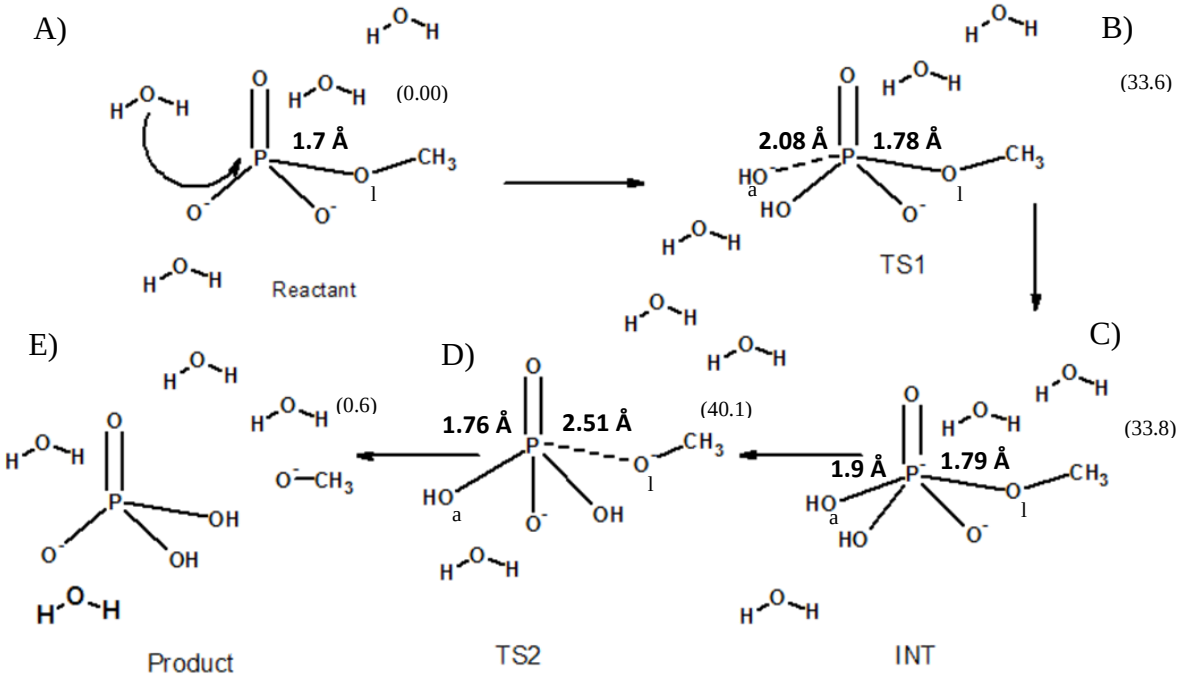

Figure 4.6 Reaction Scheme of Reaction 2, Values in parenthesis are energy values in kcal mol^{-1} relative to the reactant

Meanwhile the proton was transferred to one of the oxygen of terminal phosphate. Only one intermediate state was achieved, in which the bond distances between P-O_l increased and the P-O_a bond decreased. In the second transition state the P-O_l distance further increases and the P-O_a bond is further shortens. The final product at the end was methoxy and phosphate. Reaction 1 proceeds by P-O_a bond formation and P-O_l bond breaking (See Figure 4.7 and 4.10).

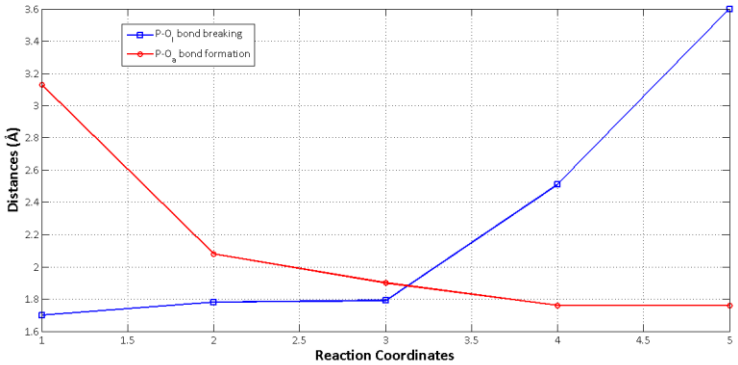

Figure 4.7 P-O_a and P-O_l bond distances of Reaction 2 from reactant to product

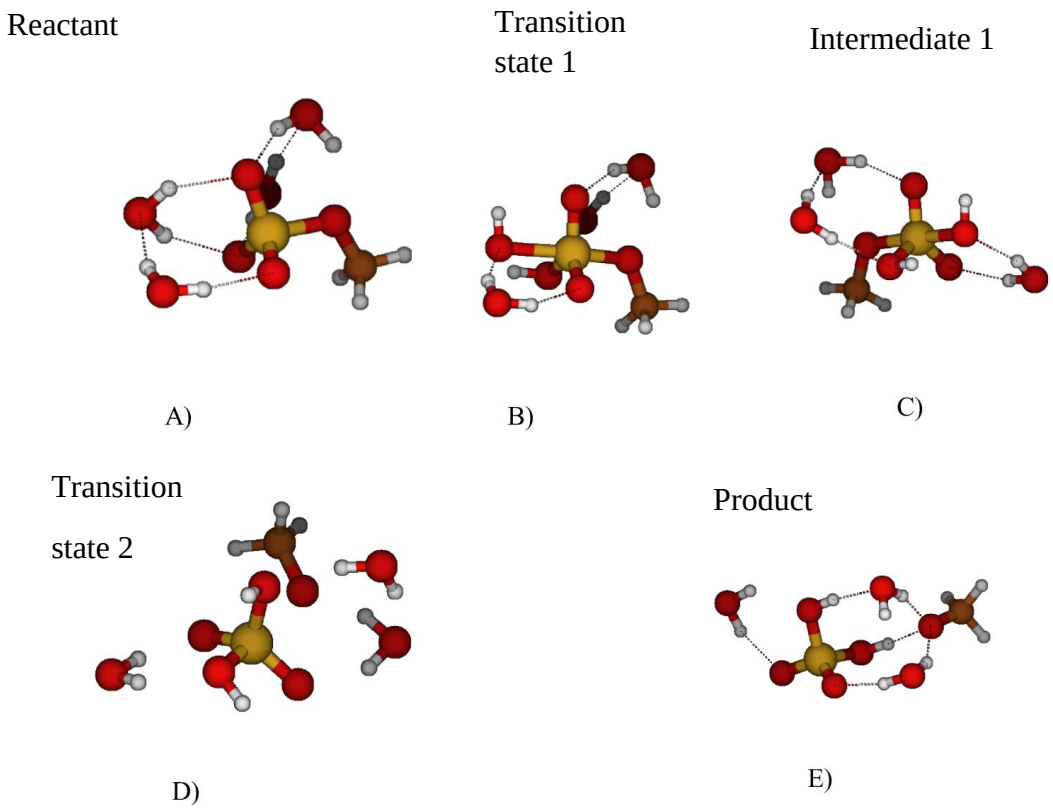

Figure 4.8 Optimized geometries of Reaction 2 A) Reactant B) TS1 C) INT D) TS2 E) Product

Table 4.2 Energies relative to the reactant (E_{rel}) of all the starting points along on reaction 2 on M06-2X/6-31+G* energy surface

Label	Stationary Points	NImag	E_{opt}[a] (Hartee)	E_{opt}[b] (Kcal mol^{-1})	E_{zpe}[c] (Kcal mol^{-1})	$E_{opt}+E_{zpe}$[d] (Kcal mol^{-1})	E_{rel}[e] (Kcal mol^{-1})
A	Reactant	0	-987.8	-619825.7	99.5	-619726.2	0.0
B	TS1	1	-987.7	-619791.3	98.7	-619692.6	33.6
C	INT	0	-987.7	-619791.4	98.9	-619692.4	33.8
D	TS2	1	-987.7	-619783.0	96.9	-619686.1	40.1
E	Product	0	-987.8	-619824.1	98.5	-619725.6	0.6

[a] The energy of optimized structures is in Hartree units.
[b] The Hartree energy was converted to kcal mol^{-1}
[c] E_{zp} is a zeropint energy which is calculated for vibrational frequencies
[d] E_{zp} added to E_{opt}
[e] E_{zp} + E_{opt} of all structures in reaction 1 relative to that of reactants

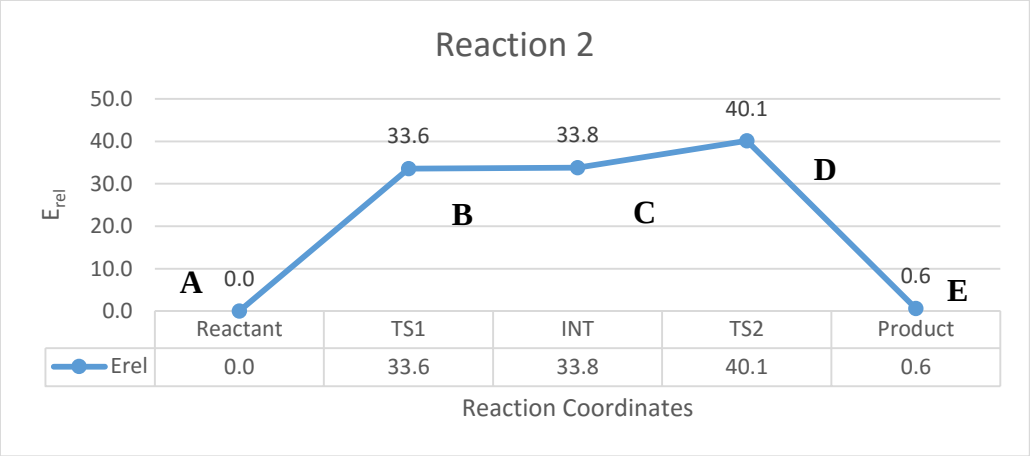

Figure 4.9 Energy profile of Reaction 2

It is a plot between relative energy (E_{rel}) and Reaction coordinates. The E_{rel} values are on y-axis and Reaction coordinates are placed on x-axis. The first transition state (TS1) is 34.4 kcal mol^{-1} higher in energy relative to the reactant. On the other hand, the intermediate have a bit lower energy than TS1 (34.4 kcal mol-^{1}). The reaction 2 has the energy barrier of 42.7 kcal mol^{-1} which is second transition state (TS2). The energy of the product is 0.6 kcal mol-^{1}. The progression of Reaction 2 according to Warshel *et al.*[38] studies shown in Figure 4.10.

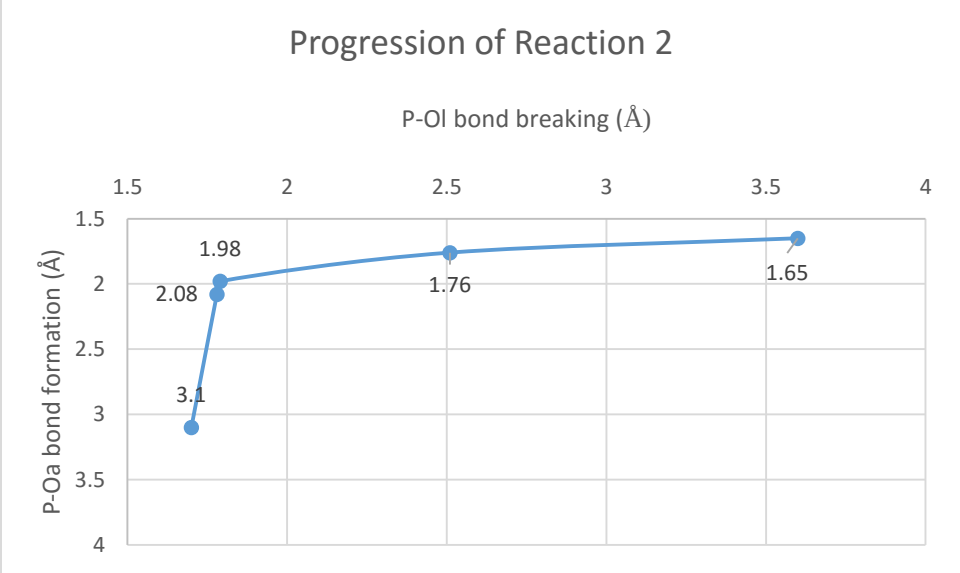

Figure 4.10 Progression of Reaction 2

4.2 Calculations of single point energies in the absence or presence of solvent for Reaction 1

Single point energies were calculated at m062x/6-31++G** level to find out how does calculating single point energies at higher basis set effect the energy profile. The energies calculated at M06-2X/6-311++G**//M06-2X/6-31+G* for the reaction 1were calculated and the results are displayed in Figure 4.11.

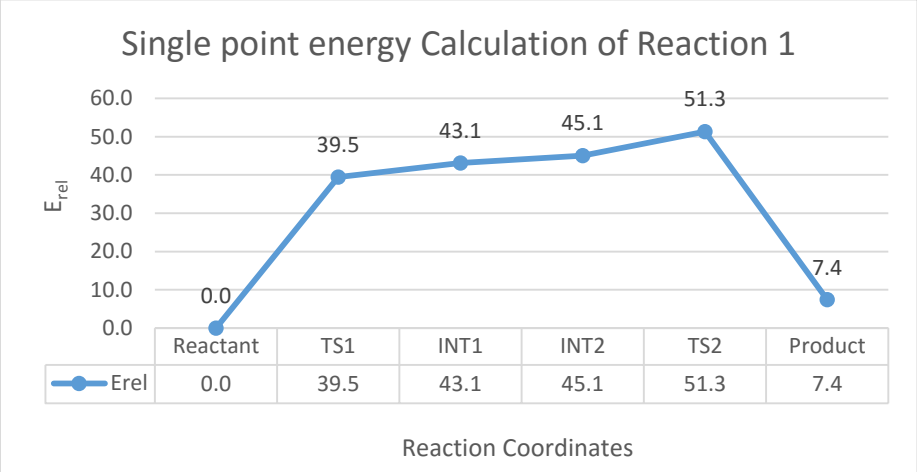

Figure 4.11 Single point energy calculations for Reaction 1

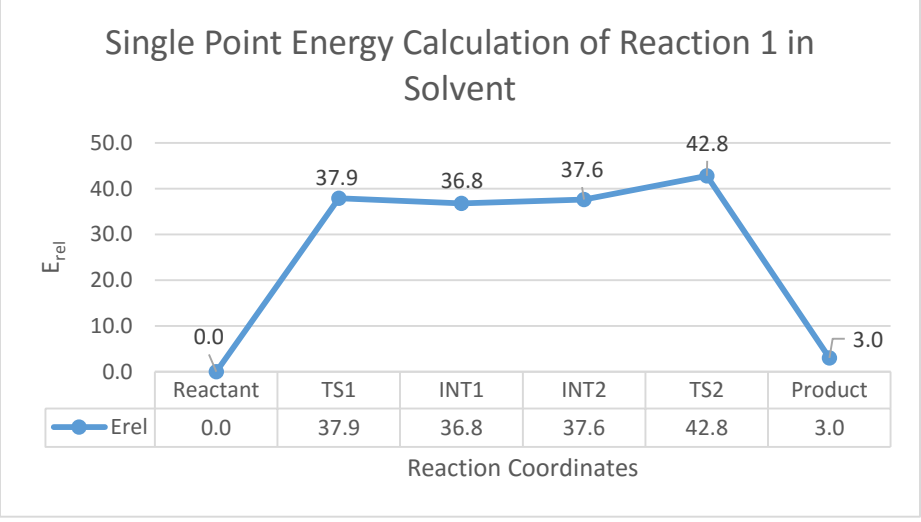

Figure 4.12 Single point energy calculation of Reaction 1 in Solvent

It is important to see that energies of all structures were high when single point energies were calculated at m062x/6-311++G** for reaction 1 (Figure 4.11). However solvent effects (Figure 4.12) seemed to have synchronisingly lowering effect as all energies are lower as compared to M06-2X/6-31+G*. These values in Figure 4.9 are also lower than the energy of the optimized structure (Figure 4.4). Thus, solvent plays an imortant role in lowering the energies because it gives stability to overall system which ultimately leads to the decrease in the energies of the optimized structures.

4.3 Calculations of single point energies in the absence or presence of solvent for Reaction 2

The single point energies of all stationary points along reaction were also calculated in the absence of solvent (Figure 4.13) and in the presence of solvent (Figure 4.14). It turns out that calculating single point energies did not much effect the energy profile of Reaction 2. One most probable reason is that reaction 2 has already one extra water as compared to setup 1 (Compare Figure 4.3 and 4.7). Moreover, this additional water in setup 2 is located more towards the P-O-C site which undergoes P-O bond breakage. This additional water provides enough stability to the system, and thus the energy barriers are not much effected by adding implicit solution.

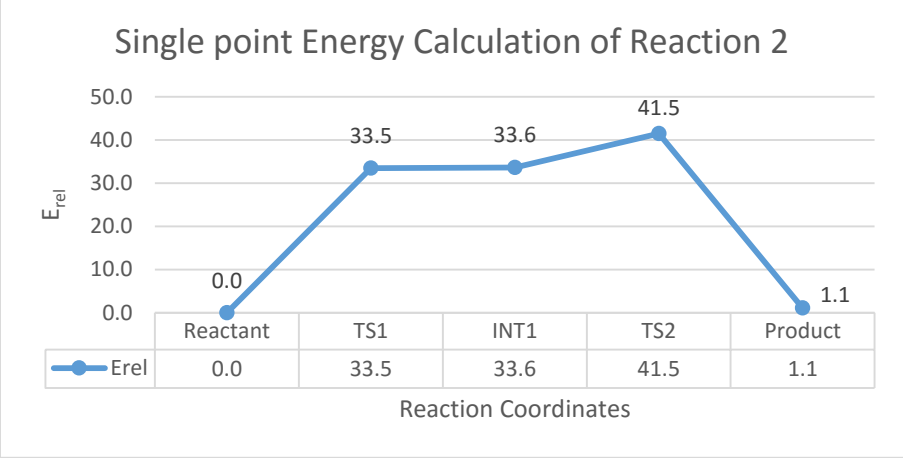

Figure 4.13 Single point energy calculation of Reaction 2

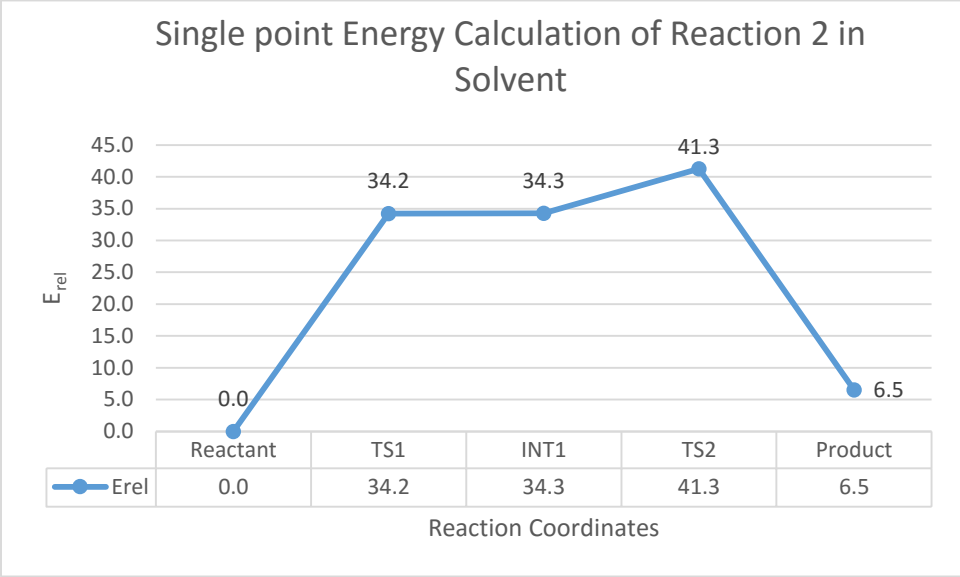

Figure 4.14 Single point energy calculation of Reaction 2 in Solvent

4.4 Reaction 1 and Reaction 2 optimized with B3LYP/6-31+G**

Geometries and relative energies of reactant, product and the rate limiting transition state of reaction 1 and reaction 2 were also calculated by using B3LYP/6-31+G**. In this approach we were able to achieve the rate limiting transition state (TS1). The transition state obtained using B3LYP/6-31+G** (see TS, Figure 4.15) strongly resembles transition state 2 (Figure 4.1 E) at M06-2X/6-31+G*. Not only structurally but also the E_{rel} values of both transition states are very similar (Compare E_{rel}=46.5 kcal mol^{-1}) for TS2 in Table 4.1 with the E_{rel}=47.2 kcal mol^{-1} of TS in Table 4.3.

There are overall three waters in the Reaction 1, But only one water involved in the hydrolysis of Methyl phosphate, which is present near the terminal phosphate. The lytic water molecule attacks on the phosphate. In this reaction the O-H bond of the lytic water molecule and the P-O_l bond breaks at the same time, which indicates that this reaction followed the concurrent mechanism.

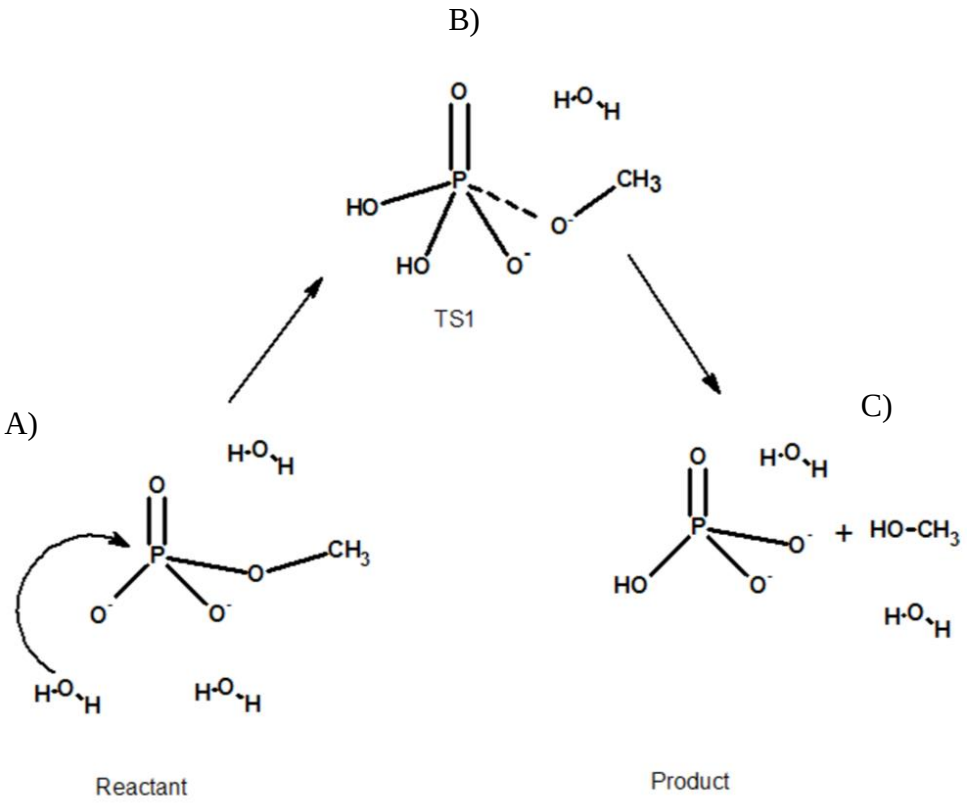

Figure 4.15 Reaction Scheme of Reaction 1 with B3LYP/6-31+G**

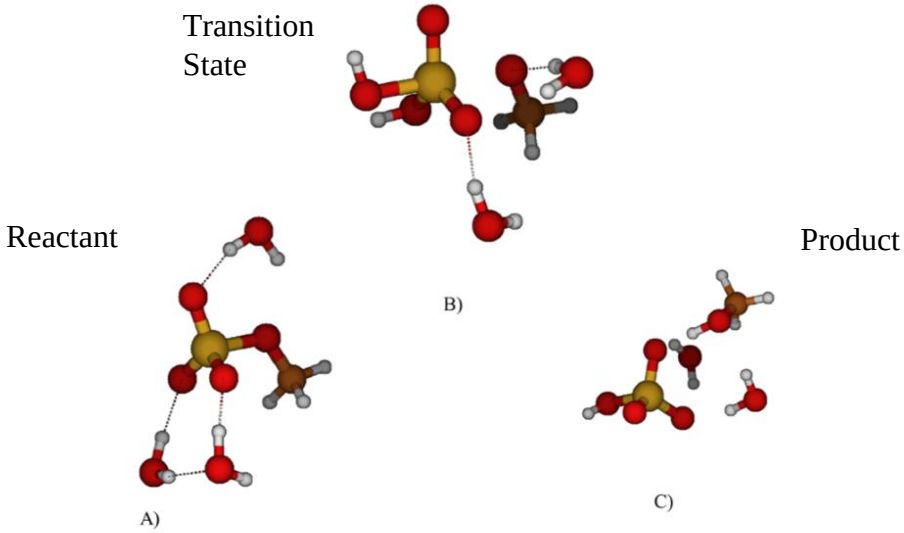

Figure 4.16 Geometries of Reaction 1 with B3LYP A) Reactant B) TS1 C) Product

Table 4.3 Energies relative to the reactant (E_{rel}) of all the starting points along on Reaction 1 with B3LYP/6-31+G**

Label	Statationary Point	Nimag	E_{opt}[a] (Hartree)	E_{opt}[b] (kcal mol^{-1})	E_{zpe}[c] (kcal mol^{-1})	$E_{opt}+E_{zpe}$[d] (kcal mol^{-1})	E_{rel}[e]
A	Reactant	0	-911.6	-572065.7	79.6	-571986.2	0.0
B	TS	1	-911.6	-572017.2	78.2	-571939.0	47.2
C	Product	0	-911.6	-572060.8	80.2	-571980.6	5.5

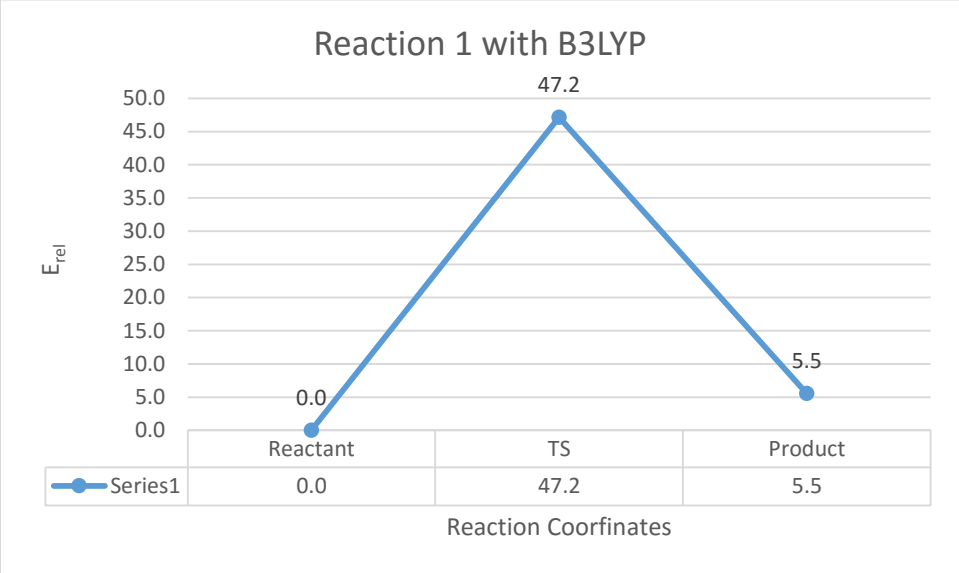

Figure 4.17 Energy profile of Reaction 1 with B3LYP

In the above plot the relative energies (E_{rel}) were placed on y-axis and Reaction Coordinates placed on y-axis. There is only one transition state achieved in this profilewhich is rate limiting transition state. The energy barrier is 48.5 kcal mol^{-1}. The finally optimized product has the energy of 4.9 kcal mol^{-1}.

[a] The energy of optimized structures is in Hartree units
[b] The Hartree energy was converted to kcal mol^{-1}
[c] E_{zp} is a zeropint energy which is calculated for vibrational frequencies
[d] E_{zp} added to E_{opt}
[e] E_{zp} + E_{opt} of all structures in reaction 1 relative to that of reactants

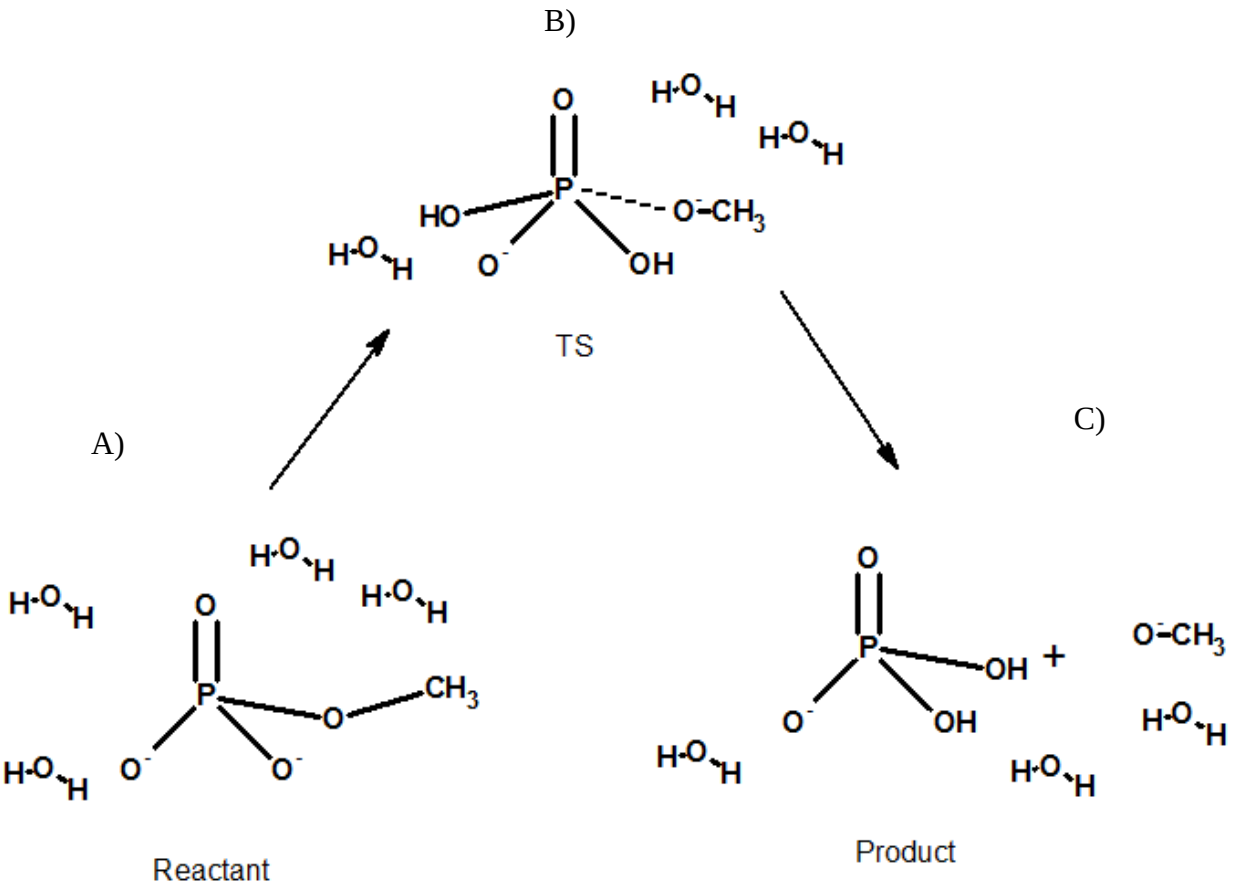

Figure 4.18 Reaction Scheme of Reaction 2 with B3LYP

We also optimized the rate limiting transition state of the reaction 2 at B3LYP/6-31+G** level of the theory. It turned out that the structures of rate limiting transition state obtained from B3LYP/6-31+G** level of theory (Figure 4.17 C) was similar to the structure obtained at M06-2X/6-31+G*. The realtive energies of the rate limiting transition state at B3LYP/6-31+G** and M06-2X/6-31+G* were also 39.0 (TS, Table 4.4) and 40.0 kcal mol^{-1} (TS, Table 4.2), which are in strong agreement with each other.

Table 4.4 Energies relative to the reactant (E_{rel}) of all the starting points along on Reaction 2 with B3LYP/6-31+G**

Labels	Stationary Points	Nimag	E_{opt}[a] (Hartree)	E_{opt}[b] (kcal mol^{-1})	E_{zpe}[c] (Kcal mol^{-1})	$E_{opt}+E_{zpe}$[d] (Kcal mol^{-1})	E_{rel}[e]
A	Reactant	0	-988.1	-620049.9	96.9	-619953.0	0.0
B	TS2	1	-988.0	-620008.5	94.4	-619914.0	39.0
C	Product	0	-988.1	-620022.2	96.5	-619925.7	27.3

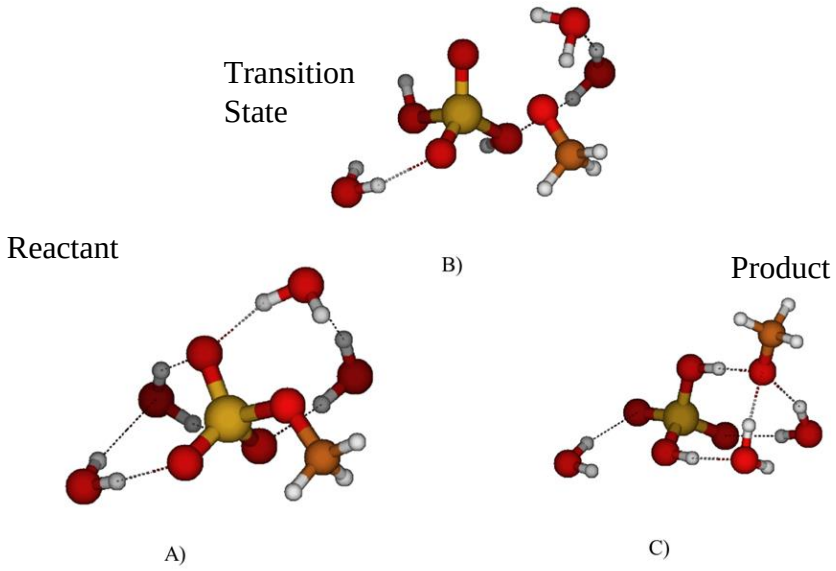

Figure 4.19 Optimized geometries of Reaction 2 with B3LYP A) Reactant B) Transition state C) Product

[a] The energy of optimized structures is in Hartree units
[b] The Hartree energy was converted to kcal mol^{-1}
[c] E_{zp} is a zeropint energy which is calculated for vibrational frequencies
[d] E_{zp} added to E_{opt}
[e] E_{zp} + E_{opt} of all structures in reaction 1 relative to that of reactants

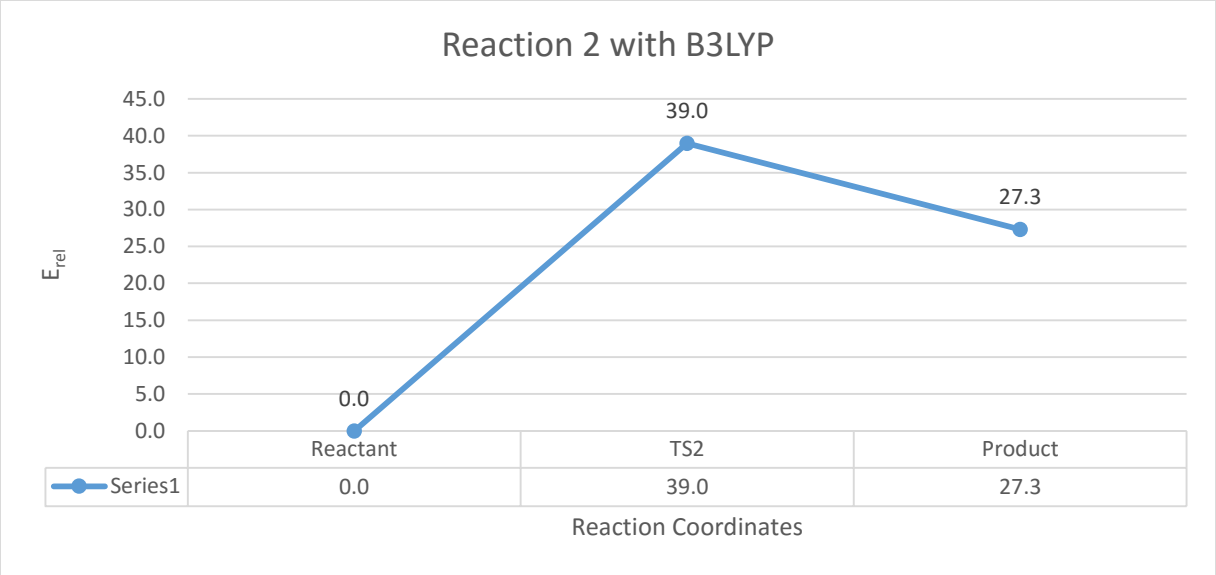

Figure 4.20 Energy profile of Reaction 2 with B3LYP

In the above plot the relative energies placed on x-axis and reaction cordinates on y-axis. The reactant has lowest energy which is 0.0 kcal mol^{-1} with single transition state and energy barrier which is about 41.5 kcal mol^{-1} The optimized product has surprisingly a high energy of 27.3 kcal mol^{-1} relative to the reactant. The optimized product which is very high energy as compared to other methods.

Chapter 5
Discussion

5. Discussion

5.1 Comparison of Reaction 1 and Reaction 2 with those of Kamerlin *et al.*[54]

5.1.1 Comparison of Reaction 1 with those of Kamerlin *et al.*[54]

In the literature, there are several studies in which quantum chemical methods have been used to study the reaction mechanism of methyl phosphate. Most studies have found both sequential and concurrent mechanisms. Contrarily, in our study single mechanism was found in which the stationary points have mixed characteristics of both sequential and concurrent mechanisms. Only one such previous study was carried out by Kamerlin *et al.*,[54] which involved the optimization of stationary points on the free energy surface in the presence of implicit and explicit solvation. Therefore it is important to compare our results (which were obtained in gas-phase) with those obtained from Kamerlin *et al.*[54]

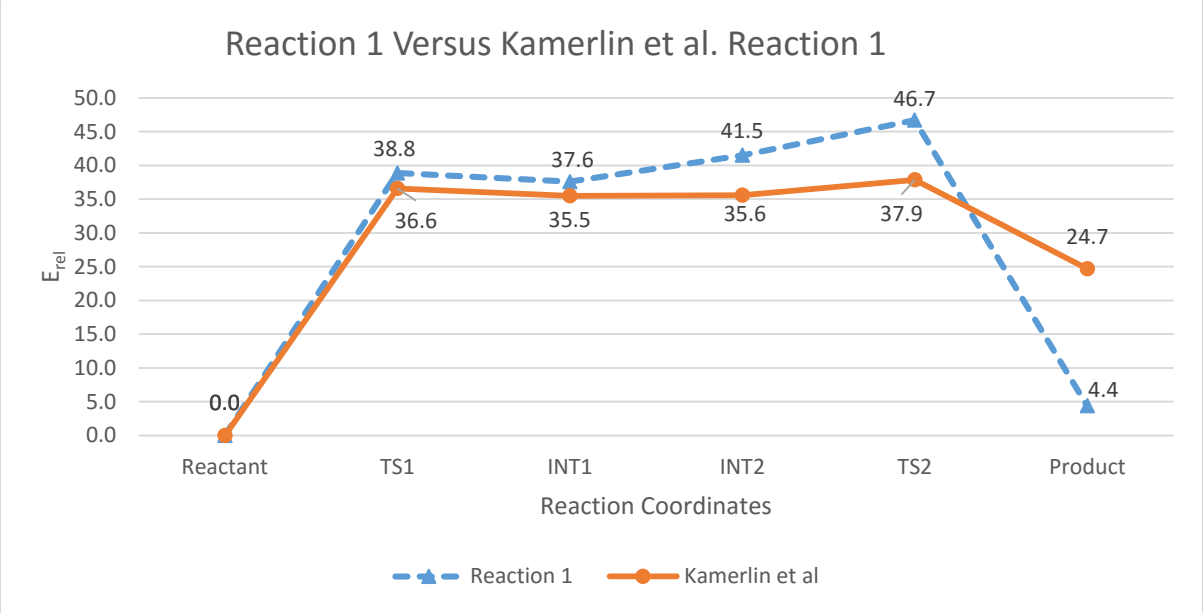

Fig 5.1 Comparison of Reaction 1 energy profile with the free energy profile reported Kamerlin *et al.*[54]

The reaction 1 has the higher rate limiting energy barrier of 46.7 kcal mol^{-1} as compared to the kamerlin *et al.*[54] (37.9 kcal mol^{-1}). It is because of the reason that kamerlin *et al.*[54] studied the phosphate monoester hydrolysis in the presence of implicit solvent and our studies took place in a gas place. However, our Reaction 1 has product with very lower energy of 4.7 kcal mol^{-1} as compared to the product of the Reaction 1 of Kamerlin *et al.*[54] with the energy of 24.7 kcal mol^{-1}. The fact behind the large difference in the energies of the final products of both the reactions is that Kamerlin *el al.*[54] had obtained a pre-product type optimized geometry of the product. However, we had obtained finally optimized structure of the final product with the transfer of proton to the methoxy group and converting it into methoxide.

5.1.2 Comparison of Reaction 2 with those of Kamerlin *et al.*[54]

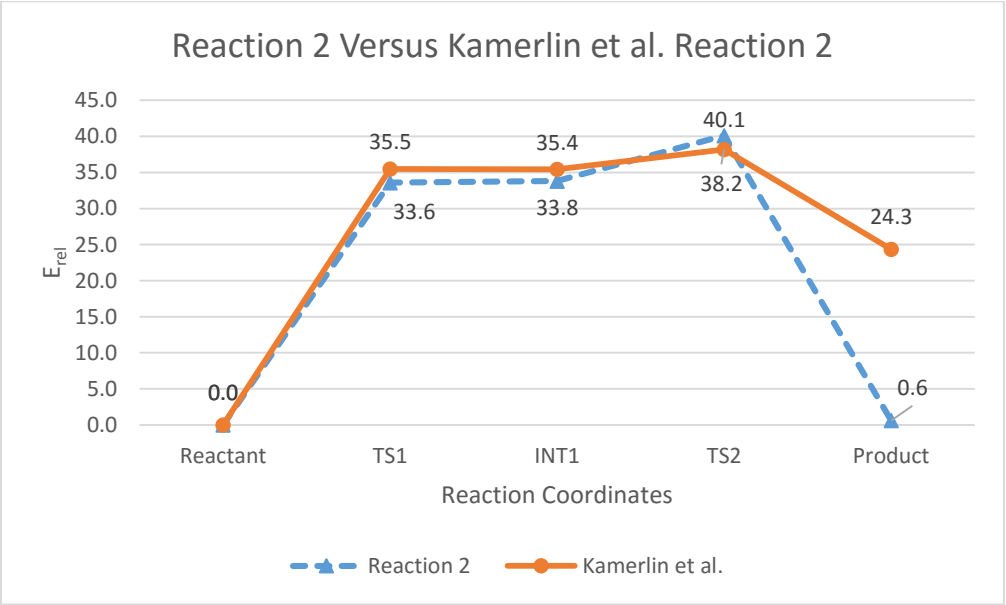

Figure 5.2 Comparison of Reaction 2 energy profile with the free energy profile reported by Kamerlin *et al.*[54]

The above plot is a comparison between Reaction 2 and the results reported by Kamerlin *et al.*,[54] The energy values of TS1 of both reactions are quite same. The energy of the TS1 of reaction 2 (35.4 kcal mol^{-1}) is slightly higher than the TS1 of the Kamerlin *et al.*[54] which is 33.8 kcal mol^{-1}. The optimized intermediate geometries of reaction 2 from our results and Kamerlin *et al.*[54] is comparable. The rate limiting energy barrier of reaction 2 (40.1 kcal mol^{-1}) is quite higher than reported by Kamerlin *et al.*[54] (38.2 kcal mol^{-1}). It is because of the reason that the current study is performed in gas phase and Kamerlin *et al.*[54] did the optimization in the solvent.

5.2 Comparison of Reaction 1 single point energy in the presence and absence of solvent

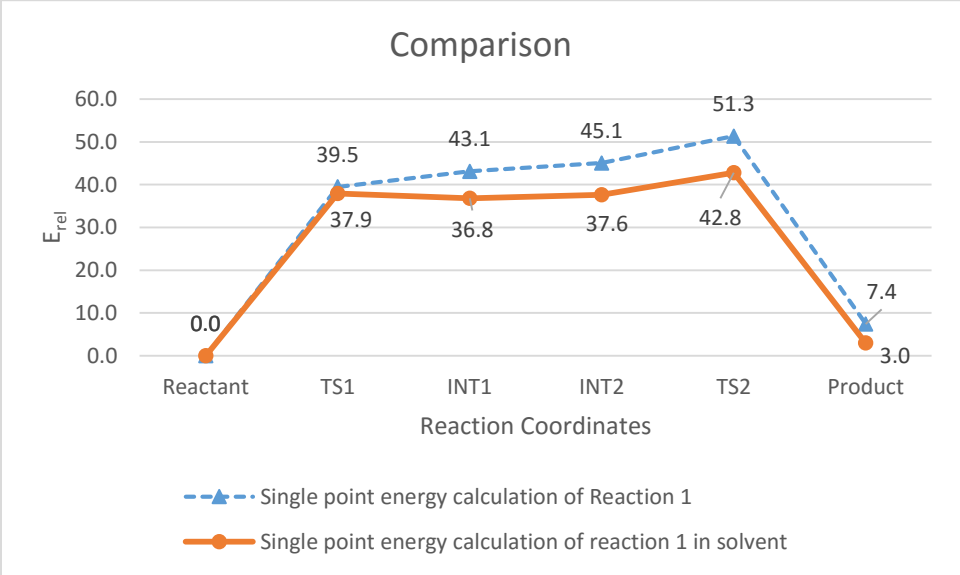

Figure 5.3 Comparison of Reaction 1 single point energy and single point energy in solvent

The above plot shows the comparison between single point energy and single point energy in solvent. The single point energy calculated in vacuum and single point energy calculated in solvent has comparable difference. The TS1 of single point energy in vacuum is 39.5 kcal mol^{-1} which is comparatively higher than the single point energy in solvent which is 37.9 kcal mol^{-1}. Solvent

facilitates the decrease in energy. The first intermediate of reaction 1 single point energy in vacuum is also higher than the first intermediate of reaction 1 single point energy in solvent. Same in the case of intermediate two in which the second intermediate of reaction 1 single point energy in vacuum has the energy value of 45.1 kcal mol^{-1} but on the other hand the single point energy in solvent for second intermediate is 37.6 kcal mol^{-1}. The energy barrier for reaction 1 single point energy calculation in vacuum is very high near 51.3 kcal mol^{-1} but for reaction 2 single point energy calculation in solvent is about 42.8 kcal mol^{-1} which very low than the former energy barrier. Interestingly, the single point energy calculation for the product achieved in the solvent is lower as compared to single point energy calculation in vacuum. The comparison is in good agreement with the findings of Kamerlin *et al.*[54] in which energy barriers are low in the presence of solvent.

5.3 Comparison of our Reaction 2 single point energy in the presence and absence of solvent

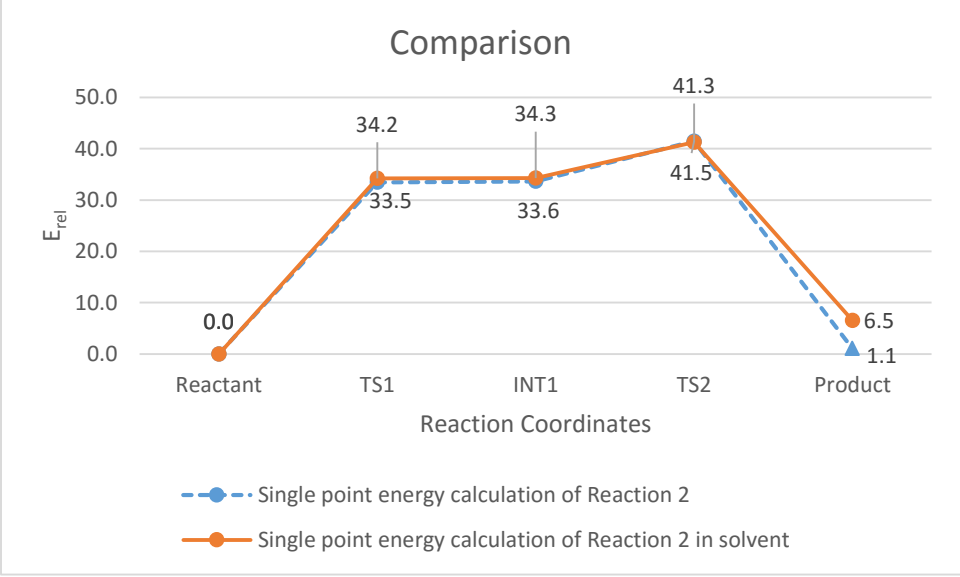

Figure 5.4 Comparison of our Reaction 2 single point energy and single point energy in solvent

The above graph describes the comparison between Reaction 2 single point energy in vacuum and Reaction 2 single point energy in solvent. The plot goes in a same manner for both cases and even it has the same energy barrier of 41.5 kcal mol^{-1}. It is due to the extra water molecules located in the Reaction 2 and when the single point energy calculated in both approaches, the results were similar even the energy barrier.

5.4 Conclusion

A minimum energy path for the hydrolysis of phosphate monoester is computed on the M06-2X potential energy surface, in the gas-phase. The stationary points along this minimum energy path have mixed characteristics of both sequential (dissociative) and concurrent (associative) mechanisms. The mechanism of phosphate monoester hydrolysis involves only one water molecule. Changing the method of density functional theory (and changing the basis set) does not significantly alter the barrier of the rate limiting transition state: The structures and relative energies of rate-limiting transition states obtained from M06-2X/6-31+G^{*} and B3LYP/6-31+G^{**} methods are comparable. This indicates the consistency of the presented results at different levels of theory. Moreover, addition of explicit solvent water molecule lowers the barrier of phosphate monoester hydrolysis. A comparison of the gas-phase calculations for reaction 1 and reaction 2 with the previously reported solvent-phase calculations reveal that the rate limiting energy barriers of phosphate monoester hydrolysis are higher in gas-phase calculations. Thus even the implicit solvent also lowers the energy barrier of phosphate monoester hydrolysis. Current calculations have been performed in the absence of surrounding protein residues. It is conceivable that barriers will be significantly lowered in the presence of enzyme.

5.5 Limitations of the study

Larger systems, *e.g*., proteins and enzymes cannot be studied using quantum chemical methods. Only the systems containing up to 100 atoms can be studied. Even smaller system are time consuming and the larger systems will ultimately be more time consuming and computationally expensive.

5.6 Future directions

Molecular dynamics and combined quantum mechanical/classical simulations of restriction endonuclease enzymes that hydrolyze phosphoester linkage is one very important area that still needs the attention of computational chemistry community. Other areas of research include investigating the effect of protonation states on the mechanism of phosphate monoester hydrolysis, and the reaction mechanism of hydrolysis of phosphodiester and phosphotriesters in gas-phase, solvent as well as in enzymes. There are several enzymes which catalyze the hydrolysis of P-O-P, P-O-C and C-OC linkages. However, the study of such larger systems was beyond the scope of this study.

Chapter 6
References

6. References

1. Reis, M.; Alves, C. N.; Lameira, J.; Tunon, I.; Marti, S.; Moliner, V., The catalytic mechanism of glyceraldehyde 3-phosphate dehydrogenase from Trypanosoma cruzi elucidated via the QM/MM approach. *Physical chemistry chemical physics : PCCP* **2013,** *15* (11), 3772-85.
2. Hou, G.; Cui, Q., QM/MM analysis suggests that Alkaline Phosphatase (AP) and nucleotide pyrophosphatase/phosphodiesterase slightly tighten the transition state for phosphate diester hydrolysis relative to solution: implication for catalytic promiscuity in the AP superfamily. *J Am Chem Soc* **2012,** *134* (1), 229-46.
3. Parks, J. M.; Hu, H.; Rudolph, J.; Yang, W., Mechanism of Cdc25B phosphatase with the small molecule substrate p-nitrophenyl phosphate from QM/MM-MFEP calculations. *J Phys Chem B* **2009,** *113* (15), 5217-24.
4. Wong, R.; Hadjiyanni, I.; Wei, H. C.; Polevoy, G.; McBride, R.; Sem, K. P.; Brill, J. A., PIP2 hydrolysis and calcium release are required for cytokinesis in Drosophila spermatocytes. *Curr Biol* **2005,** *15* (15), 1401-1406.
5. Friesner, R. A.; Guallar, V., Ab initio quantum chemical and mixed quantum mechanics/molecular mechanics (QM/MM) methods for studying enzymatic catalysis. *Annual review of physical chemistry* **2005,** *56*, 389-427.
6. Schliwa, M.; Woehlke, G., Molecular motors. *Nature* **2003,** *422* (6933), 759-765.
7. Khalili-Araghi, F.; Gumbart, J.; Wen, P. C.; Sotomayor, M.; Tajkhorshid, E.; Schulten, K., Molecular dynamics simulations of membrane channels and transporters. *Curr Opin Struct Biol* **2009,** *19* (2), 128-37.
8. Li, J. H.; King, N. C.; Sinoway, L. I., ATP concentrations and muscle tension increase linearly with muscle contraction. *J Appl Physiol* **2003,** *95* (2), 577-583.
9. McLester, J. R., Jr., Muscle contraction and fatigue. The role of adenosine 5'-diphosphate and inorganic phosphate. *Sports medicine* **1997,** *23* (5), 287-305.
10. Molina, R.; Stella, S.; Redondo, P.; Gomez, H.; Marcaida, M. J.; Orozco, M.; Prieto, J.; Montoya, G., Visualizing phosphodiester-bond hydrolysis by an endonuclease. *Nat Struct Mol Biol* **2015,** *22* (1), 65-72.
11. O'Brien, M. C.; Flaherty, K. M.; McKay, D. B., Lysine 71 of the chaperone protein Hsc70 Is essential for ATP hydrolysis. *J Biol Chem* **1996,** *271* (27), 15874-8.
12. Lohman, A. W.; Billaud, M.; Isakson, B. E., Mechanisms of ATP release and signalling in the blood vessel wall. *Cardiovasc Res* **2012,** *95* (3), 269-280.
13. Berridge, M. J.; Irvine, R. F., Inositol phosphates and cell signalling. *Nature* **1989,** *341* (6239), 197-205.
14. Narayanan, A.; Jacobson, M. P., Computational studies of protein regulation by post-translational phosphorylation. *Curr Opin Struc Biol* **2009,** *19* (2), 156-163.
15. Vale, R. D.; Milligan, R. A., The way things move: looking under the hood of molecular motor proteins. *Science* **2000,** *288* (5463), 88-95.
16. Westheimer, F. H., Why Nature Chose Phosphates. *Science* **1987,** *235* (4793), 1173-1178.
17. van der Kamp, M. W.; Mulholland, A. J., Combined quantum mechanics/molecular mechanics (QM/MM) methods in computational enzymology. *Biochemistry-Us* **2013,** *52* (16), 2708-28.
18. Senn, H. M.; Thiel, W., QM/MM studies of enzymes. *Curr Opin Chem Biol* **2007,** *11* (2), 182-187.
19. Valiev, M.; Yang, J.; Adams, J. A.; Taylor, S. S.; Weare, J. H., Phosphorylation reaction in cAPK protein kinase-free energy quantum mechanical/molecular mechanics simulations. *J Phys Chem B* **2007,** *111* (47), 13455-13464.
20. Perez-Gallegos, A.; Garcia-Viloca, M.; Gonzalez-Lafont, A.; Lluch, J. M., A QM/MM study of Kemptide phosphorylation catalyzed by protein kinase A. The role of Asp166 as a general acid/base catalyst. *Physical chemistry chemical physics : PCCP* **2015,** *17* (5), 3497-511.
21. Qian, H., Phosphorylation energy hypothesis: open chemical systems and their biological functions. *Annual review of physical chemistry* **2007,** *58*, 113-42.

22. Vijayalakshmi, P.; Selvaraj, C.; Singh, S. K.; Nisha, J.; Saipriya, K.; Daisy, P., Exploration of the binding of DNA binding ligands to Staphylococcal DNA through QM/MM docking and molecular dynamics simulation. *Journal of biomolecular structure & dynamics* **2013,** *31* (6), 561-71.
23. Ahmadian, M. R.; Stege, P.; Scheffzek, K.; Wittinghofer, A., Confirmation of the arginine-finger hypothesis for the GAP-stimulated GTP-hydrolysis reaction of Ras. *Nat Struct Biol* **1997,** *4* (9), 686-689.
24. Vetter, I. R.; Wittinghofer, A., Nucleoside triphosphate-binding proteins: different scaffolds to achieve phosphoryl transfer. *Q Rev Biophys* **1999,** *32* (1), 1-56.
25. Langen, R.; Cai, K. W.; Altenbach, C.; Khorana, H. G.; Hubbell, W. L., Structural features of the C-terminal domain of bovine rhodopsin: A site-directed spin-labeling study. *Biochemistry-Us* **1999,** *38* (25), 7918-7924.
26. Glennon, T. M.; Villa, J.; Warshel, A., How does GAP catalyze the GTPase reaction of Ras?: A computer simulation study. *Biochemistry-Us* **2000,** *39* (32), 9641-9651.
27. Dittrich, M.; Hayashi, S.; Schulten, K., QM/MM study of ATP hydrolysis in the tight binding pocket of F-1-ATPase. *Biophys J* **2003,** *84* (2), 456a-456a.
28. Dittrich, M.; Schulten, K., PcrA helicase, a prototype ATP-driven molecular motor. *Structure* **2006,** *14* (9), 1345-53.
29. Akola, J.; Jones, R. O., ATP hydrolysis in water - A density functional study. *J Phys Chem B* **2003,** *107* (42), 11774-11783.
30. Florian, J.; Warshel, A., Quantum-chemical insights into mechanisms of the nonenzymatic hydrolysis of phosphate monoesters. *Phosphorus Sulfur* **1999,** *144*, 525-528.
31. Florian, J.; Warshel, A., Phosphate ester hydrolysis in aqueous solution: Associative versus dissociative mechanisms. *J Phys Chem B* **1998,** *102* (4), 719-734.
32. Kiani, F. A.; Fischer, S., Catalytic strategy used by the myosin motor to hydrolyze ATP. *P Natl Acad Sci USA* **2014,** *111* (29), E2947-E2956.
33. Grigorenko, B. L.; Nemukhin, A. V.; Topol, I. A.; Cachau, R. E.; Burt, S. K., QM/MM modeling the Ras-GAP catalyzed hydrolysis of guanosine triphosphate. *Proteins* **2005,** *60* (3), 495-503.
34. Grigorenko, B. L.; Rogov, A. V.; Nemukhin, A. V., Mechanism of triphosphate hydrolysis in aqueous solution: QM/MM simulations in water clusters. *J Phys Chem B* **2006,** *110* (9), 4407-4412.
35. Glaves, R.; Mathias, G.; Marx, D., Mechanistic Insights into the Hydrolysis of a Nucleoside Triphosphate Model in Neutral and Acidic Solution. *J Am Chem Soc* **2012,** *134* (16), 6995-7000.
36. Kiani, F. A.; Fischer, S., Advances in quantum simulations of ATPase catalysis in the myosin motor. *Curr Opin Struc Biol* **2015,** *31*, 115-123.
37. Kiani, F. A.; Fischer, S., Stabilization of the ADP/Metaphosphate Intermediate during ATP Hydrolysis in Pre-power Stroke Myosin QUANTITATIVE ANATOMY OF AN ENZYME. *J Biol Chem* **2013,** *288* (49), 35569-35580.
38. Kamerlin, S. C. L.; Sharma, P. K.; Prasad, R. B.; Warshel, A., Why nature really chose phosphate. *Q Rev Biophys* **2013,** *46* (1), 1-132.
39. Hu, C. H.; Brinck, T., Theoretical studies of the hydrolysis of the methyl phosphate anion. *J Phys Chem A* **1999,** *103* (27), 5379-5386.
40. Lecocq, J., Methyl triphosphate, a substrate for myosin adenosine triphosphatase. *Journal of medicinal chemistry* **1968,** *11* (5), 1096-7.
41. Jelenc, P. C.; Kurland, C. G., Nucleoside triphosphate regeneration decreases the frequency of translation errors. *Proc Natl Acad Sci U S A* **1979,** *76* (7), 3174-8.
42. Forti, G.; Meyer, E. M., Effect of pyrophosphate on photosynthetic electron transport reactions. *Plant Physiol* **1969,** *44* (11), 1511-4.
43. Ishida, A.; Toraya, T., Adenosylcobinamide methyl phosphate as a pseudocoenzyme for diol dehydrase. *Biochemistry-Us* **1993,** *32* (6), 1535-40.
44. Schliwa, M.; Woehlke, G., Molecular motors. *Nature* **2003,** *422* (6933), 759-65.
45. Wang, W.; Cao, L.; Wang, C.; Gigant, B.; Knossow, M., Kinesin, 30 years later: Recent insights from structural studies. *Protein science : a publication of the Protein Society* **2015,** *24* (7), 1047-56.

46. Itoh, H.; Takahashi, A.; Adachi, K.; Noji, H.; Yasuda, R.; Yoshida, M.; Kinosita, K., Mechanically driven ATP synthesis by F1-ATPase. *Nature* **2004,** *427* (6973), 465-8.
47. Lightstone, F. C.; Zheng, Y. J.; Maulitz, A. H.; Bruice, T. C., Non-enzymatic and enzymatic hydrolysis of alkyl halides: a haloalkane dehalogenation enzyme evolved to stabilize the gas-phase transition state of an SN2 displacement reaction. *Proc Natl Acad Sci U S A* **1997,** *94* (16), 8417-20.
48. Wang, Y. N.; Topol, I. A.; Collins, J. R.; Burt, S. K., Theoretical studies on the hydrolysis of mono-phosphate and tri-phosphate in gas phase and aqueous solution. *J Am Chem Soc* **2003,** *125* (43), 13265-13273.
49. Wang, C.; Huang, W. T.; Liao, J. L., QM/MM Investigation of ATP Hydrolysis in Aqueous Solution. *J Phys Chem B* **2015,** *119* (9), 3720-3726.
50. Harrison, C. B.; Schulten, K., Quantum and Classical Dynamics Simulations of ATP Hydrolysis in Solution. *J Chem Theory Comput* **2012,** *8* (7), 2328-2335.
51. Klahn, M.; Rosta, E.; Warshel, A., On the mechanism of hydrolysis of phosphate monoesters dianions in solutions and proteins. *J Am Chem Soc* **2006,** *128* (47), 15310-15323.
52. Prasad, B. R.; Plotnikov, N. V.; Warshel, A., Addressing Open Questions about Phosphate Hydrolysis Pathways by Careful Free Energy Mapping. *J Phys Chem B* **2013,** *117* (1), 153-163.
53. Florian, J.; Warshel, A., A fundamental assumption about OH- attack in phosphate ester hydrolysis is not fully justified. *J Am Chem Soc* **1997,** *119* (23), 5473-5474.
54. Duarte, F.; Aqvist, J.; Wiliams, N. H.; Kamerlin, S. C. L., Resolving Apparent Conflicts between Theoretical and Experimental Models of Phosphate Monoester Hydrolysis. *J Am Chem Soc* **2015,** *137* (3), 1081-1093.
55. Yang, Y.; Cui, Q., The Hydrolysis Activity of Adenosine Triphosphate in Myosin: A Theoretical Analysis of Anomeric Effects and the Nature of the Transition State. *J Phys Chem A* **2009,** *113* (45), 12439-12446.
56. Abrahams, J. P.; Leslie, A. G.; Lutter, R.; Walker, J. E., Structure at 2.8 A resolution of F1-ATPase from bovine heart mitochondria. *Nature* **1994,** *370* (6491), 621-8.
57. Dittrich, M.; Hayashi, S.; Schulten, K., ATP hydrolysis in the betaTP and betaDP catalytic sites of F1-ATPase. *Biophys J* **2004,** *87* (5), 2954-67.
58. Dittrich, M.; Schulten, K., Zooming in on ATP hydrolysis in F1. *Journal of bioenergetics and biomembranes* **2005,** *37* (6), 441-4.
59. Hayashi, S.; Ueno, H.; Shaikh, A. R.; Umemura, M.; Kamiya, M.; Ito, Y.; Ikeguchi, M.; Komoriya, Y.; Iino, R.; Noji, H., Molecular Mechanism of ATP Hydrolysis in F-1-ATPase Revealed by Molecular Simulations and Single-Molecule Observations. *J Am Chem Soc* **2012,** *134* (20), 8447-8454.
60. McGrath, M. J.; Kuo, I. F. W.; Hayashi, S.; Takada, S., Adenosine Triphosphate Hydrolysis Mechanism in Kinesin Studied by Combined Quantum-Mechanical/Molecular-Mechanical Metadynamics Simulations. *J Am Chem Soc* **2013,** *135* (24), 8908-8919.
61. Ma, B. Y.; Xie, Y. M.; Shen, M. Z.; Schaefer, H. F., Po3(-).(H2o)N Clusters - Molecular Anion Structures, Energetics, and Vibrational Frequencies. *J Am Chem Soc* **1993,** *115* (5), 1943-1951.
62. Zhao, Y.; Truhlar, D. G., The M06 suite of density functionals for main group thermochemistry, thermochemical kinetics, noncovalent interactions, excited states, and transition elements: two new functionals and systematic testing of four M06-class functionals and 12 other functionals. *Theor Chem Acc* **2008,** *120* (1-3), 215-241.
63. Petersson, G. A.; Bennett, A.; Tensfeldt, T. G.; Allaham, M. A.; Shirley, W. A.; Mantzaris, J., A Complete Basis Set Model Chemistry .1. The Total Energies of Closed-Shell Atoms and Hydrides of the 1st-Row Elements. *J Chem Phys* **1988,** *89* (4), 2193-2218.
64. Petersson, G. A.; Allaham, M. A., A Complete Basis Set Model Chemistry .2. Open-Shell Systems and the Total Energies of the 1st-Row Atoms. *J Chem Phys* **1991,** *94* (9), 6081-6090.
65. Petersson, G. A.; Tensfeldt, T. G.; Montgomery, J. A., A Complete Basis Set Model Chemistry .3. The Complete Basis Set-Quadratic Configuration-Interaction Family of Methods. *J Chem Phys* **1991,** *94* (9), 6091-6101.

66. Schaftenaar, G.; Noordik, J. H., Molden: a pre- and post-processing program for molecular and electronic structures. *J Comput Aid Mol Des* **2000,** *14* (2), 123-134.
67. Cossi, M.; Rega, N.; Scalmani, G.; Barone, V., Energies, structures, and electronic properties of molecules in solution with the C-PCM solvation model. *J Comput Chem* **2003,** *24* (6), 669-681.

Appendix A: Cartesian coordinates of the optimized geometries in reaction 1 and reaction 2

Reaction 1

Reactant

P	-0.431408	-0.524919	0.207516
O	-0.962650	0.987918	-0.439338
O	-1.758989	-1.179694	0.565811
O	0.444170	-0.101871	1.408226
O	0.370644	-1.151406	-0.934959
C	0.068870	1.853880	-0.808639
O	3.039982	-0.707663	-1.301750
H	2.069538	-0.929622	-1.252074
H	3.193612	-0.341552	-0.409944
H	0.843372	1.330462	-1.390104
H	-0.354013	2.662351	-1.425750
H	0.542987	2.308718	0.078471
H	-3.017369	1.107051	-0.361990
O	-3.767173	0.555858	-0.076413
H	-3.229400	-0.220410	0.233077
H	1.923224	0.272581	1.340131
O	2.884516	0.653497	1.260756
H	2.726623	1.511161	0.844623

Transition state 1

P	0.025705	-0.401585	-0.158383
O	0.831023	1.157798	0.075446
O	1.313001	-1.215344	-0.224735
O	-0.874919	-0.041063	-1.331753
O	-0.724522	-0.218638	1.324441
C	0.018692	2.288366	0.111761
O	-1.011933	-2.286217	0.162059
H	-1.097323	-1.142999	1.363909
H	-0.216483	-2.835433	0.156712
H	-0.605648	2.316105	1.021259
H	0.663631	3.184555	0.110686
H	-0.653062	2.330046	-0.758011
H	2.808799	1.030303	0.174248
O	3.516981	0.361405	0.112520
H	2.905330	-0.405533	-0.033877
H	-2.465590	0.539838	-0.708069
O	-3.108024	0.901808	-0.042481
H	-2.590564	0.701029	0.757079

Reaction 2

Reactant

P	0.249317	-0.459288	-0.117977
O	-1.278044	-1.222706	-0.061794
O	0.086763	0.469486	-1.335855
O	1.272162	-1.579268	-0.252797
O	0.322121	0.317665	1.214707
C	-1.500471	-1.990211	1.092510
O	2.013335	2.127369	-0.110713
H	1.549306	1.706008	0.648218
H	1.435422	1.786748	-0.829322
H	-1.545931	-1.350954	1.984836
H	-2.459210	-2.515356	0.972817
H	-0.699166	-2.731790	1.226237
H	-2.587245	0.118769	-0.840119
O	-2.562819	1.016608	-1.218838
H	-1.584403	1.050409	-1.402411
H	2.968583	-0.842393	-0.320752
O	3.767407	-0.260088	-0.347521
H	3.364957	0.626615	-0.274238
H	-1.176746	1.212939	1.587002
O	-2.062250	1.659063	1.639269
H	-2.347868	1.638644	0.706824

Transition state 1

P	-0.367100	-0.045933	-0.139402
O	0.969644	1.064496	-0.528564
O	0.304039	-1.268961	-0.767437
O	-1.502317	0.777943	-0.719326
O	-0.012110	0.227167	1.481376
C	0.776220	2.408518	-0.215565
O	-1.696374	-1.347306	0.798291
H	-0.627958	-0.410658	1.897036
H	-1.348610	-2.168316	0.425526
H	0.705454	2.566783	0.873593
H	1.638994	2.984196	-0.590558
H	-0.144095	2.793644	-0.679103
H	2.603921	0.139258	-1.008046
O	2.935521	-0.780860	-1.005307
H	2.034849	-1.208377	-0.973384
H	-3.320025	0.276010	-0.557863
O	-4.001077	-0.322102	-0.177734
H	-3.348072	-0.901307	0.291891
H	1.854689	-0.044305	1.799604
O	2.803848	-0.284352	1.863534
H	3.001751	-0.552344	0.943398

Intermediate 1

C	0.004493	2.190093	0.116471
O	0.790696	1.049302	0.127709
P	-0.039862	-0.559047	-0.140760
O	-0.777471	-0.254540	1.367409
O	1.316482	-1.283387	-0.210665
O	-0.904108	-0.092263	-1.318248
O	-0.920182	-2.220803	0.049479
O	3.470145	0.341601	0.056176
O	-3.135429	0.849232	-0.080690
H	-1.223370	-1.105338	1.518175
H	-0.158169	-2.811958	-0.008701
H	-0.644729	2.262100	1.010455
H	0.661429	3.081654	0.112279
H	-0.646522	2.230041	-0.770683
H	2.740606	0.986251	0.150594
H	2.863687	-0.434423	-0.081023
H	-2.462042	0.482079	-0.719692
H	-2.605468	0.753073	0.729471

Intermediate 2

P	-0.143694	-0.709909	0.190174
O	1.095267	0.306323	1.074625
O	0.592022	-1.998373	0.537209
O	-0.028909	0.079407	-1.142359
O	-1.273784	-0.003753	1.244430
C	0.900163	1.682832	1.097102
O	-1.671518	-1.681301	-0.374839
H	-2.069220	-0.510193	1.008208
H	-1.329161	-2.577214	-0.258666
H	0.070996	1.974056	1.768824
H	1.822118	2.171330	1.465772
H	0.683317	2.089409	0.095815
H	2.582931	0.258681	-0.301027
O	2.711296	0.487213	-1.243781
H	1.760574	0.403768	-1.502932
H	-1.180482	1.289932	-1.113794
O	-1.875704	2.020745	-1.096549
H	-2.142120	1.960386	-0.167127

Intermediate

P	0.347908	0.011008	0.135762
O	-1.063165	1.118750	-0.001595
O	-0.237110	-0.723475	1.349771
O	1.422080	1.089264	0.131991
O	-0.119290	-0.572295	-1.380963
C	-0.979856	2.127570	-0.956209
O	1.676374	-1.455395	-0.067358
H	0.507796	-1.308583	-1.497361
H	1.410668	-1.993399	0.690316
H	-0.962433	1.720859	-1.982160
H	-1.867115	2.777661	-0.862888
H	-0.072826	2.734510	-0.814003
H	-2.601626	0.532747	1.000979
O	-2.872670	-0.263297	1.501770
H	-1.945453	-0.612955	1.624974
H	3.234961	0.678786	0.089810
O	3.967747	0.023471	0.017761
H	3.369387	-0.759685	-0.022154
H	-1.975356	-1.037465	-1.351459
O	-2.901482	-1.327825	-1.207919
H	-3.039582	-1.083790	-0.270002

Transition state

P	-0.541047	-0.176915	-0.158878
O	1.285304	1.126887	-0.027881
O	0.184988	-0.887222	-1.294295
O	-1.393648	1.071817	-0.240300
O	0.035747	-0.494657	1.390127
C	1.216953	2.137339	0.890456
O	-1.756035	-1.353133	0.057041
H	-0.534817	-1.202219	1.722340
H	-1.523720	-2.023557	-0.600373
H	1.402902	1.796189	1.936821
H	1.972029	2.936098	0.690962
H	0.222694	2.628815	0.891053
H	2.510101	0.441138	-0.912676
O	2.905022	-0.322555	-1.432790
H	2.039084	-0.747839	-1.623995
H	-3.177501	0.862741	-0.092514
O	-4.021121	0.356496	0.033195
H	-3.611633	-0.524467	0.094597
H	1.969457	-0.862536	1.359222
O	2.844190	-1.295951	1.273919
H	3.058499	-1.074331	0.342953

Transition State 2

P	-0.726710	-0.596430	0.032354
O	1.484577	-0.180033	1.037677
O	-0.527314	-2.003738	0.514778
O	-0.160682	0.021870	-1.231303
O	-1.019860	0.572950	1.186936
C	1.833485	1.135386	1.061246
O	-2.438686	-0.667705	-0.349924
H	-1.963734	0.760692	1.072234
H	-2.655447	-1.579091	-0.111225
H	1.171298	1.757225	1.716845
H	2.874748	1.312242	1.448232
H	1.810733	1.620580	0.055971
H	2.289257	-0.754018	-0.281500
O	2.581932	-0.917906	-1.240366
H	1.735872	-0.668348	-1.655182
H	-0.510899	1.823932	-1.228169
O	-0.657510	2.721245	-0.836973
H	-0.422522	2.510044	0.082622

Product

C	2.312372	1.268148	1.320865
O	1.886660	-0.038400	1.607879
P	-1.167121	-0.715929	-0.174142
O	-2.734336	-0.110835	-0.430089
O	-1.424569	-2.170357	0.193314
O	-0.413340	-0.433445	-1.489402
O	-0.603796	0.180255	0.970655
O	2.307452	-0.934409	-1.177598
O	-0.135140	2.299760	-0.854092
H	0.882243	-0.058237	1.400903
H	-3.285812	-0.864324	-0.180268
H	2.011924	1.981258	2.111105
H	3.411383	1.273938	1.262998
H	1.907938	1.631036	0.366600
H	2.295564	-0.811377	-0.210072
H	1.350539	-0.803199	-1.406381
H	-0.141448	1.481117	-1.401055
H	-0.368111	1.870377	-0.002040

Product

C	2.129510	2.446856	0.433951
O	1.714404	1.214328	0.008490
P	-1.434205	-0.284027	-0.895610
O	-1.423623	-0.885406	0.646757
O	-0.497484	-1.136347	-1.730926
O	-2.892116	-0.161621	-1.272139
O	-0.816955	1.200308	-0.724312
O	2.237754	-1.034150	-1.509455
O	1.307317	-1.063673	1.250622
O	-4.275213	-1.023983	0.968241
H	0.173739	1.198431	-0.496300
H	-0.493091	-1.037802	0.939065
H	2.926843	2.393597	1.211526
H	2.552758	3.070097	-0.387189
H	1.309197	3.051784	0.880323
H	2.275816	-0.130939	-1.118737
H	1.274046	-1.119900	-1.720881
H	-4.029702	-0.678123	0.076067
H	-3.374130	-1.144403	1.316031
H	1.478277	-0.108059	0.987619
H	1.618260	-1.512246	0.441081